Towards robust and replicable sex differences in the intrinsic brain function of autism

Dorothea L. Floris*[1,2], José O. A. Filho*[3], Meng-Chuan Lai[4,5,6,7,8], Steve Giavasis[3], Marianne Oldehinkel[9], Maarten Mennes[1], Tony Charman[10], Julian Tillmann[10,21], Guillaume Dumas[11], Christine Ecker[12,13], Flavio Dell'Acqua[12,14], Tobias Banaschewski[15], Carolin Moessnang[16], Simon Baron-Cohen[7], Sarah Durston[17], Eva Loth[12,14], Declan G. M. Murphy[12,14], Jan K. Buitelaar[1,2,18], Christian F. Beckmann[1,2,19], Michael P. Milham[3,20], Adriana Di Martino[3]

***equal contribution**

[1] Donders Center for Brain, Cognition and Behavior, Radboud University Nijmegen, Nijmegen, The Netherlands

[2] Department for Cognitive Neuroscience, Radboud University Medical Center Nijmegen, Nijmegen, The Netherlands

[3] Child Mind Institute, New York City, New York, USA

[4] The Margaret and Wallace McCain Centre for Child, Youth & Family Mental Health, Azrieli Adult Neurodevelopmental Centre, and Campbell Family Mental Health Research Institute, Centre for Addiction and Mental Health, Toronto, Canada

[5] Department of Psychiatry and Autism Research Unit, The Hospital for Sick Children, Toronto, Canada

[6] Department of Psychiatry, Faculty of Medicine, University of Toronto, Toronto, Canada

[7] Autism Research Centre, Department of Psychiatry, University of Cambridge, Cambridge, United Kingdom

[8] Department of Psychiatry, National Taiwan University Hospital and College of Medicine, Taipei, Taiwan

[9] Turner Institute for Brain and Mental Health, School of Psychological Sciences, Monash University, Victoria, Australia

[10] Department of Psychology, Institute of Psychiatry, Psychology, and Neuroscience, King's College London, London, United Kingdom

[11] Human Genetics and Cognitive Functions, Institut Pasteur, UMR3571 CNRS, Université de Paris, Paris, France

[12] Sackler Institute for Translational Neurodevelopment, Institute of Psychiatry, Psychology, and Neuroscience, King's College London, London, United Kingdom

[13] Department of Child and Adolescent Psychiatry, Psychosomatics and Psychotherapy, University Hospital Frankfurt am Main, Goethe University, Frankfurt, Germany

[14] Department of Forensic and Neurodevelopmental Sciences, Institute of Psychiatry, Psychology, and Neuroscience, King's College London, London, United Kingdom

[15] Child and Adolescent Psychiatry, Department of Psychiatry and Psychotherapy, Central Institute of Mental Health, University of Heidelberg, Mannheim, Germany

[16] Department of Psychiatry and Psychotherapy, Central Institute of Mental Health, University of Heidelberg, Mannheim, Germany

[17] Department of Psychiatry, Brain Center Rudolf Magnus, University Medical Center Utrecht, Utrecht, the Netherlands

[18] Karakter Child and Adolescent Psychiatry University Centre, Nijmegen, the Netherlands

[19] Centre for Functional MRI of the Brain, University of Oxford, Oxford, United Kingdom

[20] Nathan Kline Institute for Psychiatric Research, Orangeburg, New York, USA

[21] Department of Applied Psychology: Health, Development, Enhancement, and Intervention, University of Vienna, Vienna, Austria

Corresponding author:

Adriana Di Martino, MD

Child Mind Institute,

Autism Center

101 E 56 Street

NY, NY 10026

Email: Adriana.Dimartino@childmind.org

Keywords

Autism spectrum disorder, resting-state functional connectivity, sex differences, replication, robustness, voxel-mirrored homotopic connectivity

ORCID IDs:

Floris DL: https://orcid.org/0000-0001-5838-6821

Filho JOA: https://orcid.org/0000-0001-8471-8594

Lai M-C: https://orcid.org/0000-0002-9593-5508

Mennes M: https://orcid.org/0000-0002-7279-3439

Charman T: https://orcid.org/0000-0003-1993-6549

Tillmann J: https://orcid.org/0000-0001-9574-9855

Dumas G: https://orcid.org/0000-0002-2253-1844

Dell'Acqua F: https://orcid.org/0000-0001-5313-5476

Banaschewski T: https://orcid.org/0000-0003-4595-1144

Moessnang C: https://orcid.org/0000-0003-4357-2706

Baron-Cohen S: https://orcid.org/0000-0001-9217-2544

Murphy DGM: https://orcid.org/0000-0002-6664-7451

Buitelaar JK: https://orcid.org/0000-0001-8288-7757

Beckmann CF: https://orcid.org/0000-0002-3373-3193

Milham MP: https://orcid.org/0000-0003-3532-1210

Di Martino A: https://orcid.org/0000-0001-6927-290X

Abstract

Background: Marked sex differences in autism prevalence accentuate the need to understand the role of biological sex-related factors in autism. Efforts to unravel sex differences in the brain organization of autism have, however, been challenged by the limited availability of female data. **Methods**: We addressed this gap by using a large sample of males and females with autism and neurotypical (NT) control individuals (ABIDE; Autism: 362 males, 82 females; NT: 409 males, 166 females; 7-18 years). Discovery analyses examined main effects of diagnosis, sex and their interaction across five resting-state fMRI (R-fMRI) metrics (voxel-level $Z > 3.1$, cluster-level $P < 0.01$, gaussian random field corrected). Secondary analyses assessed the robustness of the results to different pre-processing approaches and their replicability in two independent samples: the EU-AIMS Longitudinal European Autism Project (LEAP) and the Gender Explorations of Neurogenetics and Development to Advance Autism Research (GENDAAR). **Results**: Discovery analyses in ABIDE revealed significant main effects across the intrinsic functional connectivity (iFC) of the posterior cingulate cortex, regional homogeneity and voxel-mirrored homotopic connectivity (VMHC) in several cortical regions, largely converging in the default network midline. Sex-by-diagnosis interactions were confined to the dorsolateral occipital cortex, with reduced VMHC in females with autism. All findings were robust to different pre-processing steps. Replicability in independent samples varied by R-fMRI measures and effects with the targeted sex-by-diagnosis interaction being replicated in the larger of the two replication samples – EU-AIMS LEAP. **Limitations**: Given the lack of *a priori* harmonization among the discovery and replication datasets available to date, sample-related variation remained and may have affected replicability. **Conclusions**: Atypical cross-hemispheric interactions are neurobiologically relevant to autism. They likely result from the combination of sex-

dependent and sex-independent factors with a differential effect across functional cortical networks. Systematic assessments of the factors contributing to replicability are needed and necessitate coordinated large-scale data collection across studies.

Background

Autism spectrum disorder (autism) is characterized by a marked male preponderance in prevalence with three times more males being diagnosed than females [1]. This pronounced sex-differential prevalence implies that sex-related biological factors are likely implicated in the neurobiology of autism. However, little is known about the differential underlying neural expressions in males and females with autism. Such knowledge could widen our understanding of potential underlying mechanisms of autism and related neurodevelopmental conditions [2].

This has motivated research into the impact of biological sex on brain organization in autism [2–5]. With the widely accepted view that the neurobiology of autism involves differences in large-scale brain networks [6,7], resting-state functional magnetic resonance imaging (R-fMRI) has proven to be a valuable complementary tool for investigating atypicalities in intrinsic functional connectivity (iFC). While the exact nature of the intrinsic brain organization in autism remains to be established [6], research on the impact of biological sex differences in autism is just beginning to emerge.

Several R-fMRI studies have focused on autism-related sex differences in iFC [2,8,17,18,9–16]. They vary on the extent of the functional networks and intrinsic properties examined. Most of them examined the strength of iFC between one or more regions/networks selected *a priori* [8–10,12,13,17,18], or via data-driven analyses [16]. A few others investigated either local or homotopic iFC across the whole brain [2,11,15]. Across these different efforts, the pattern of findings have also been mixed; some studies supported the predictions from the 'extreme male brain theory' [10,11], others supported the predictions from the 'gender-

136 incoherence' theory [8,9,12,13,16]. The extreme male brain theory model predicts that brain
137 characteristics in males and females with autism will resemble those in neurotypical males
138 (i.e., shifts towards maleness in both sexes [19]). R-fMRI results consistent with a shift
139 towards maleness in autism were reported in both Ypma et al. [10] and Kozhemiako et al.
140 [11,15]. The 'gender incoherence' model predicts that brain characteristics in females with
141 autism resemble those of neurotypical males, whereas brain characteristics in males with
142 autism resemble those of neurotypical females (i.e., androgynous patterns in the sexes [20]).
143 The 'gender incoherence' model has been supported by findings from prior R-fMRI studies
144 [8,9,12], where the results largely revealed hyper-connectivity in females with autism similar
145 to neurotypical (NT) males and hypo-connectivity in males with autism similar to NT
146 females. Such seemingly inconsistent findings of sex-related differences were in part
147 addressed by Floris et al. [2] who showed that, at least in males with autism, distinct patterns
148 of atypical sex-differentiation coexist, and vary as a function of the neural networks involved.
149 However, the intrinsic brain organization in females with autism has remained largely unclear
150 and the scarce availability of female datasets in most studies may have contributed to the
151 variability in findings in males and females [21,22].
152
153 Accordingly, to explore sex-related atypicalities in autism relative to NT controls, we used, as
154 discovery sample, a large R-fMRI datasets of both males and females of autism and NT
155 selected from the Autism Brain Imaging Data Sharing Exchange (ABIDE) [22,23]. By
156 aggregating neuroimaging datasets from multiple sources, this data sharing initiative has
157 begun to provide a means to address the challenge of underrepresentation of female datasets
158 in autism research. Examining both sexes in both autism and controls allows to directly
159 capture not only sex differences that are common across individuals (i.e., regardless of their
160 diagnosis [main effect of sex]), but also those that are specific to autism and point towards

161 atypical autism-specific sex differential patterns (i.e., sex-by-diagnosis interaction effects)
162 [4]. To do so, given prior inconsistencies in the literature and the limited insights onto the
163 brain organization of females with autism, we used a discovery approach. Unlike most prior
164 work that focused on specific networks or circuits selected *a priori*, we investigated the
165 whole-brain across multiple R-fMRI metrics. We selected R-fMRI metrics capturing unique
166 aspects of the intrinsic brain organization during typical development [24,25] and, most
167 germane to this study, being reported to be involved in typical sex differences and be affected
168 by autism. They comprised: 1) posterior cingulate cortex (PCC)-iFC – e.g., [2,10,23,26–32];
169 2) voxel-mirrored homotopic connectivity (VMHC) [33] – e.g., [11,32–35]; 3) regional
170 homogeneity (ReHo) [36] – e.g., [15,32,37,38]; 4) network degree centrality (DC) [39] – e.g.,
171 [32,39–41]; and 5) fractional amplitude of low frequency fluctuations (fALFF) [23,42] – e.g.,
172 [23,32,43].
173
174 Beside the role of small female samples, prior inconsistencies in autism-related sex
175 differences in R-fMRI can be due to other factors that can impact reproducibility. For
176 example, while there are growing concerns on the role of pre-processing strategies [44,45], a
177 recent study showed that their impact on autism-related mean group-differences is minimal
178 [46]. Additionally, while several studies have reported some degree of consistency on R-
179 fMRI findings across either independent, or partially overlapping, samples [41,47–49], results
180 from other studies have raised concerns on the replicability of group-mean diagnostic effects
181 [46,50]. However, none of these studies have explicitly examined robustness and replicability
182 of sex-by-diagnosis interaction effects, which account for a potentially relevant source of
183 variability in autism – biological sex. Thus, we conducted secondary analyses to assess the
184 extent to which the pattern of findings obtained in our discovery analyses were also observed
185 *a)* after applying different nuisance pre-processing steps that have been previously validated,

though used inconsistently in the autism literature [46], and *b)* across two independent, multisite R-fMRI datasets: the EU-AIMS Longitudinal European Autism Project (LEAP) [51,52] and the Gender Explorations of Neurogenetics and Development to Advance Autism Research (GENDAAR) dataset [53] – i.e., *robustness* and *replicability*.

Methods

Discovery sample: ABIDE I and II

For discovery analyses, we examined the R-fMRI dataset with one of the largest number of females and males in both the autism and the NT groups available to date, selected from the Autism Brain Imaging Data Exchange (ABIDE) repositories ABIDE I and II [22,23]. The final ABIDE I and II dataset of N=1,019 included N=82 females with autism, N=362 males with autism, N=166 neurotypical females (NT F), and N=409 neurotypical males (NT M), aggregated across 13 sites. Specific selection criteria are described in Supplementary Material in the Additional file 1 and depicted as a figure in the Additional file 2. Briefly, we selected cases between 7-18 years of age (the ages most represented across ABIDE sites), with MRI data successfully completing brain image co-registration and transformation to standard space, with FIQ between 70-148 and with mean framewise displacement (mFD) [54] within three times the interquartile range (IQR) + the third quartile (Q3) of the sample (i.e., 0.39 mFD). Further steps included matching for mean age *across* groups as well as for mFD and IQ *within* diagnostic groups. This latter step limited the number of exclusions while keeping average group motion low (mFD<.2mm) and sampling biases that may result when matching neurodevelopmental conditions to NT around intrinsic features such as IQ [55,56]. At each step, any sites with less than three individual datasets per diagnostic/sex groups were

210 excluded. Demographics and characteristics of this sample are summarized in Table 1 and in
211 Supplementary Material in the Additional file 1.
212
213 **[TABLE 1]**
214
215 **Discovery analysis pre-processing pipeline**
216 We examined five whole-brain R-fMRI metrics previously reported to reflect typical sex
217 differences and found to be atypical in autism, including 1) PCC-iFC, 2) VMHC, 3) ReHo, 4)
218 DC and 5) fALFF (see Supplementary Material, Additional file 1). R-fMRI image pre-
219 processing steps included: slice time correction, 24 motion parameters regression [57],
220 component-based noise reduction (CompCor) [58], removal of linear and quadratic trends,
221 and band-pass filtering (0.01-0.1 Hz, for all metrics but fALFF). Functional-to-anatomical
222 co-registration was achieved by Boundary Based Registration (BBR) using FSL FLIRT [59].
223 Linear and nonlinear spatial normalization of functional echo planar images (EPIs) to
224 Montreal Neurological Institute 152 (MNI152) stereotactic space ($2mm^3$ isotropic) was done
225 using ANTS registration (Advanced Neuroimaging Tools) [60]. Computation of voxel-
226 mirrored homotopic connectivity (VMHC) followed registration to a symmetric template. All
227 R-fMRI derivatives were smoothed by a 6mm FWHM Gaussian kernel. To account for site
228 and collection time variability across each of the data collections in ABIDE I and II data
229 repositories, site effects were removed using the ComBat function available in python [61]
230 (https://github.com/Jfortin1/ComBatHarmonizationhttps://github.com/brentp/combat.py).
231 This approach has been shown to effectively account for scanner-related variance in multi-
232 site R-fMRI data [61]. For further details see Supplementary Material in the Additional file 1.
233
234 **Discovery group-level analyses**

Statistical Z-maps were generated within study-specific functional volume masks including all voxels in MNI space present across all subjects. Main effects of diagnosis and sex along with their interaction were explored by fitting a general linear model (GLM) including diagnosis or/and sex as the regressors of interest respectively, and age and mean framewise displacement (mFD) [54] as nuisance covariates. In primary analyses, we did not include FIQ as a covariate as this is thought to be suboptimal when comparing groups selected from populations carrying intrinsic IQ differences such as autism and NT [56]. Nevertheless, to provide an indication as to whether IQ may affect primary findings, in supplementary analyses FIQ was also included as an additional nuisance regressor. We applied gaussian random field theory correction based on strict voxel-level threshold of $Z>3.1$ as recommended by [62] and cluster level, $P<0.01$, given the assessment of five R-fMRI metrics in the same study (i.e., P 0.05/5 R-MRI metrics=0.01).

Functional relevance of sex differences in autism

Post-hoc analyses were conducted to functionally characterize the sex-by-diagnosis interaction result(s). First, to explore the cognitive domains implicated in the cluster(s), we quantified the percentage of its overlap with 12 cognitive ontology maps [63] thresholded at P=1e−5. We labelled these components based on the top five tasks each component recruits [2]. Second, we used the Neurosynth Image Decoder (http://neurosynth.org/decode/) [64] to visualize the terms most strongly associated with the significant cluster. After excluding anatomical (e.g., occipital) and redundant terms (synonyms [e.g., saccades and eye movements], plurals [e.g., object and objects] or noun/adjective/adverb equivalents [e.g., vision and visual]), we visualized the top 27 terms showing correlations with the cluster map between r=0.64 and r=0.10. Third, to explore potential clinical relevance of the significant cluster, we explored brain-behavior relationships as a function of sex within the autism

group. Specifically, we ran a GLM examining the interaction between biological sex and available ADOS calibrated severity total score (CSS) [65], as well as social-affect (SA) and restricted, repetitive behavior (RRB) subscores (see Supplementary Material, Additional file 1) with the dependent variable(s) being the R-fMRI metric(s) extracted from the cluster mask(s) showing a statistically significant sex-by-diagnosis effect(s).

Robustness and Replicability

Robustness. We assessed whether patterns of results from the discovery analyses were observable with two other nuisance regression analytical pipelines that include commonly used data preprocessing steps. One pipeline included global signal regression (GSR) [66] which has often been used in autism studies; the other included Independent Component Analysis - Automatic Removal of Motion Artifacts (ICA-AROMA) [67] which is a relatively novel but increasingly utilized approach [46]. Given the scope of the present study, unlike prior work focusing on a wide range of individual preprocessing pipelines [46], we selected GSR and ICA-AROMA as examples of previously validated approaches thought to have impact on motion and physiological noise [45]. To assess robustness of the results observed in discovery analyses, following the voxel-level GLM, we extracted means from the masks corresponding to the same clusters that showed significant effects. These values were averaged across all the voxels in the cluster mask for a given R-fMRI metric. We used them to implement a full regression model including the predictors of interest (sex, diagnosis and their interaction), as well as age and mFD as nuisance regressors and compute effect sizes as partial eta squared (η_p^2) and their confidence intervals using the R-package 'effectsize'. For visualization purposes we also used regressions (including sex, diagnosis, sex-by diagnosis, age, and mFD) to obtain the residuals of these mask-averaged values.

Replicability. Similarly, we assessed whether the group patterns observed in significant clusters identified in discovery analyses, were observed in two relatively large-scale, independent datasets selected from *a)* the EU-AIMS Longitudinal European Autism Project (LEAP), a large multi-site European initiative aimed at identifying biomarkers in autism [51,52] and *b)* the Gender Explorations of Neurogenetics and Development to Advance Autism Research (GENDAAR) dataset collected by the GENDAAR consortium and shared in the National Database for Autism Research [53]. For details on autism and NT inclusion and exclusion criteria for these samples, as well as our selection process, see Supplementary Material in the Additional file 1 [52,53]. The resulting EU-AIMS LEAP (N=309) R-fMRI datasets comprised N=133 males and N=43 females with autism as well as N=85 NT males, and N=48 NT females (see Table S1, Additional file 3); resulting GENDAAR (N=196) R-fMRI datasets comprised N=43 males and N=44 females with autism, as well as N=56 NT males and N=53 NT females (see Table S2, Additional file 3). For a comparison of demographic and clinical information between ABIDE, EU-AIMS LEAP and GENDAAR, see Table S3, S4 and S5 in the Additional file 3. After applying the same ComBat and pre-processing pipeline as used in the ABIDE-based discovery analyses, we extracted each of the R-fMRI metrics means from the Z-maps. As for robustness, we extracted values for each R-fMRI metric from the masks corresponding to the clusters showing statistically significant effects in discovery analyses and computed the corresponding effect size and residuals using the same methods described above.

For both robustness and replicability discovery findings were determined to be robust and/or replicable (R+) based on two criteria: *1)* the group mean difference(s) observed were in the same direction as those identified in the findings from discovery analyses [68] and *2)* their effects were not negligible as defined by partial eta squared η_p^2 <0.01 [69] (i.e., any small,

medium or large effects) which is also consistent with prior work [41]. Finally, for consistency across analyses we also computed cluster level effect size of the discovery findings using the same approach described above.

Results

Discovery analyses – ABIDE

Main effect of diagnosis. Analyses revealed a total of seven clusters showing a significant effect of diagnosis (voxel-level $Z>3.1$; cluster-level $P<0.01$, corrected) for three of the five R-fMRI metrics: PCC-iFC (three clusters), VMHC (two clusters) and ReHo (two clusters); Figure 1, Additional file 4. These were mainly evident in anterior and posterior regions of the default network (DN) across at least two or all three R-fMRI metrics. Autism-related hypo-connectivity was present for: a) PCC-iFC, VMHC and ReHo within bilateral paracingulate cortex and frontal pole, b) VMHC and ReHo in the bilateral PCC and precuneus, and c) ReHo in right insula and central operculum (Figure 1, Additional file 4 and Additional file 5). Autism-related hyper-connectivity was only evident for PCC-iFC with left superior lateral occipital cortex, temporal occipital fusiform cortex and occipital fusiform gyrus (see Additional file 4). These results remained essentially unchanged when additionally controlling for FIQ (Additional file 6). Further, to verify that these findings were not driven by particular acquisition site(s), post-hoc analyses computed group means for diagnostic subgroups for the R-fMRI metrics extracted at the cluster-level masks excluding one out of the 13 ABIDE sites at a time. The pattern of results was essentially unchanged (Additional file 7a).

335 ***Main effect of sex***. Analyses revealed clusters showing statistically significant main sex
336 differences (voxel-level $Z>3.1$; cluster-level $P<0.01$, corrected), again for three R-fMRI
337 metrics out of five in a total of 10 clusters: PCC-iFC (five clusters), VMHC (three clusters),
338 and ReHo (two clusters). Findings involved lateral and medial portions of the DN with
339 bilateral PCC and precuneus showing the highest overlap (see Figure 1 and Additional file 4).
340 Specifically, regardless of diagnosis, relative to females, males showed decreased PCC-iFC
341 with paracingulate cortex and frontal pole, right middle frontal gyrus, bilateral superior lateral
342 occipital cortex and bilateral PCC and precuneus. Males also showed decreased VMHC and
343 ReHo localized in PCC and precuneus. Decreased ReHo was also evident in the left angular
344 gyrus and lateral occipital cortex in females relative to males (Figure 1, Additional file 4, and
345 Additional file 5). These results remained essentially unchanged when additionally
346 controlling for FIQ (see Additional file 6). Post-hoc analyses assessing the consistency of
347 these findings across sites, as described above, revealed a similar pattern of results
348 (Additional file 7b).
349
350 ***Sex-by-diagnosis interaction***. Statistically corrected voxel-wise analyses (voxel-level $Z>3.1$;
351 cluster-level $P<0.01$) revealed one cluster of significant sex-by-diagnosis interaction only for
352 VMHC which was localized in the dorsolateral occipital cortex (Figure 2a and Additional file
353 5). Post-hoc cluster-level group means showed that NT females had higher VMHC than the
354 three other groups, whereas autism females had lower VMHC than the three other groups
355 (Figure 2a). Similar to the main effects, results remained essentially unchanged when
356 additionally controlling for FIQ (Additional file 6) and analyses assessing the consistency of
357 these findings across sites, as described above, showed a similar pattern of results (Additional
358 file 8).
359

Functional relevance of autism-related sex differences

Post-hoc analyses to functionally characterize this VMHC sex-by-diagnosis interaction indicated that the VMHC cluster in superior lateral occipital cortex overlapped with cognitive maps involved in higher-order visual, oculomotor, cognitive flexibility and language-related processes (Figure 3a). Further, as shown in Figure 3b, the most common terms were primarily related to lower-order visual processing and higher-order visual cognition, such as 'visuospatial' and 'spatial attention.' To explore potential clinical relevance of the VMHC dorsolateral occipital cluster, we explored brain-behavior relationships as a function of sex, within the autism group using three available ADOS scores (calibrated severity total score, and non-calibrated social affect and RRB subscores; see Supplementary Material in Additional file 1). Although not surviving a strict Bonferroni correction for multiple testing (i.e., 0.05/3=0.02), an interaction effect was observed for ADOS social affect scores. It revealed that more severe social deficits ($F_{(1,311)}$=4.44, p=0.036) were associated with decreased VMHC in females with autism (r=-0.29), but not in males with autism (r=0.03). Given that ABIDE data were aggregated and released when calibrated social affect scores [70] were not available to assess potential differences in language abilities and age, analyses were repeated after including ADOS module (ADOS Module 2 to 4) as a nuisance covariate: results remained unchanged ($F_{(1,306)}$=5.0, p=0.026) as they did also after removing the few data with the less represented ADOS module 2 (see Supplementary Material, Additional file 1). There were no significant findings, with regard to the CSS total score and non-calibrated RRB sub-score (Figure 3c), even at an exploratory statistical threshold of P<0.05.

Robustness

The same pattern of results identified in discovery analyses was observed in the results pre-processed using GSR or ICA-AROMA, across the three R-fMRI metrics in all the clusters

identified in the primary analyses across main effects of diagnosis, sex and their interaction; effect size ranges from small to moderate as in discovery analyses (η_p^2 range=0.01–0.07; Figure 2b, Figure 4, Additional file 5, Additional file 9).

Replicability

Main effects of diagnosis. Main effects of diagnosis showed higher replicability (i.e., non-negligible η_p^2 effects showing a similar group mean pattern as observed in discovery analyses) in GENDAAR than in EU-AIMS LEAP. Specifically, across the three R-fMRI metrics that showed significant diagnostic differences in discovery analyses, six of the seven clusters (86%) in GENDAAR, were replicated (η_p^2 range=0.01–0.04); only two of those seven (29%) were replicated in EU-AIMS LEAP (η_p^2 range=0.01–0.04). Nevertheless, clusters showing decreased ReHo in ASD vs. NT across the insula and central operculum, as well as in the frontal pole were replicated across all samples (Figure 4, Additional file 5, Additional file 10a).

Main effects of sex. Across all three R-fMRI metrics, the main effects of sex observed in primary discovery analyses was evident in both independent samples, for most clusters in the EU-AIMS LEAP (80%; 8/10) with effects size ranging from small to moderate (η_p^2 range=0.01–0.06) and for half of the clusters in GENDAAR (50%; 5/10), albeit with small effects (η_p^2 range=0.01–0.02); Figure 4, Additional file 5, Additional file 10b). Notably, the pattern of typical sex differences localized along the default network midline (i.e., decreased VMHC, ReHo and PCC-iFC) was replicated across both independent samples (Figure 4b).

Sex-by-diagnosis interaction effect. The pattern of autism-related VMHC sex differences observed in discovery analyses in the superior lateral occipital cortex was observed in the

EU-AIMS LEAP dataset, (η_p^2 =0.01); (Figure 2c, Figure 4, Additional file 5). In the GENDAAR dataset, while group means in males with autism, NT males and NT females showed a similar direction as in the ABIDE discovery findings, females with autism differed in magnitude and in the direction of group differences, resulting in a negligible effect with η_p^2<0.01. (Figure 2c).

Discussion

We examined autism-related sex differences for intrinsic functional brain organization across multiple R-fMRI metrics in a large discovery sample of males and females with autism relative to age-group matched NT selected from the ABIDE repositories [22,23]. Analyses revealed significant main effects of sex and diagnosis across intrinsic functional connectivity (iFC) of the posterior cingulate cortex, regional homogeneity and voxel-mirrored homotopic connectivity (VMHC) in several cortical regions. Notably, main effects converged along the midline of the default network. In contrast, sex-by-diagnosis interactions were limited to VMHC in the superior lateral occipital cortex. Placed in the context of sex and diagnostic main effects on interhemispheric homotopic connectivity in cortical regions, this result, suggests that atypical interhemispheric interactions are pervasive in autism but reflect a combination of sex-independent (i.e., main effect of diagnosis common across both sexes) and sex-dependent (i.e., sex-by-diagnosis interaction) effects, each specific to different functional cortical system. This sex-by-diagnosis interaction effect was robust to distinct pre-processing strategies as those observed for main effects. Further, despite the lack of *a priori* harmonization for data acquisition among the three samples, this finding was replicable in the larger of the two independent samples (i.e., EU-AIMS LEAP). On the one hand, this, together with largely replicable main effects of sex with variable replicability of main diagnostic effects by sample, suggests that inter-sample replicability of R-fMRI can be feasible in

autism when sources of variability in diagnostic groups are accounted for in samples sized properly to address such variability. On the other hand, our results highlight the urgent need to obtain multiple harmonized datasets properly powered to systematically address and understand sources of heterogeneity, including and beyond the role of biological sex.

Sex-dependent and independent atypical interhemispheric interactions in autism

VMHC reflects inter-hemispheric homotopic relations. Its strength has been suggested to index coordinated cross-hemispheric processing: *stronger* VMHC index weaker hemispheric specialization and vice versa [33,71]. Several lines of evidence support the notion that the neurobiology of autism is related to atypical hemispheric interactions, including homotopic connectivity and hemispheric lateralization [35,72,81,73–80]. VMHC and functional hemispheric lateralization have also been shown to be sex-differential in NT [33,82,83]. The dorsolateral occipital association cortex identified in our discovery analyses is known to serve hemispherically specialized processes, such as visuospatial coordination [84]. Thus, our findings of NT males' VMHC in dorsolateral lateral occipital cortex being lower than NT females are consistent with the notion of increased hemispheric lateralization in this cortical region in NT males relative to NT females. In our data, females with autism instead showed even lower VMHC than NT males, while males with autism showed slightly higher VMHC than NT males. This pattern is indicative of 'gender-incoherence' [20] as males and females with autism display the opposite pattern expected in NT per their biological sex. Findings of 'gender incoherence' have been reported in earlier neuroimaging studies of autism using different modalities [3,85,86]. Among them, several R-fMRI studies explicitly focusing on detecting diagnosis-by-sex interactions (i.e., the regression model included a sex-by-diagnosis interaction term) [3,9] yielded a pattern of results consistent with 'gender incoherence.' In contrast, other studies [10–12] reported a pattern consistent with the

460 'extreme male brain theory' [19] – i.e., a shift towards maleness in both females and males
461 with autism. While the seemingly diverging conclusions of these two sets of studies may be
462 attributed to methodological differences, such as the extent of brain networks explored and
463 the statistical modelling employed, findings from our prior work suggest that both shifts
464 towards either maleness or femaleness co-occur in the intrinsic brain of males with autism, in
465 a network-specific manner [2]. However, such prior work did not include female data. Thus,
466 by not directly assessing sex-by-diagnosis interactions, unlike the present study, results could
467 not point to patterns affecting diagnostic differences between the sexes vs. those that are
468 common to autism across both sexes [4]. This is relevant for efforts focusing on identifying
469 underlying mechanisms. Findings resulting from sex-by-diagnosis interactions may shed light
470 on sex differential mechanisms that go awry in autism and may reflect sex-specific
471 susceptibility mechanisms. On the other hand, diagnostic atypicalities common for both sexes
472 may reflect factors central to the emergence of autism, regardless of whether they overlap
473 with patterns known to be differential between sexes [87]. Interestingly, a recent study based
474 on a sample selected from GENDAAR [14] revealed that the iFC between the nucleus
475 accumbens (selected *a priori*) and a region of the dorsolateral occipital cortex partially
476 overlapping with that identified by our VMHC analyses, was differentially modulated by the
477 aggregate number of oxytocin receptor risk alleles in females with autism vs. NT females and
478 vs. males with autism. Although VMHC was not directly tested in that earlier study [14], its
479 result in dorsolateral occipital cortex is consistent with our observation of atypical sexual
480 differentiation of this visual network region and, together, suggest the need for future whole-
481 brain studies of oxytocin effects in autism.
482
483 Along with the sex-dependent autism patterns, our analyses found statistically significant
484 main effects of diagnosis in inter-hemispheric interactions indexed by VMHC in distinct

485 cortical circuits. These were localized along the midline of the DN (paracingulate/frontal
486 cortex consistently and PCC/precuneus) where main effects of PCC-iFC and ReHo also
487 converged. Our results are consistent with prior reports of atypical intrinsic organization of
488 the DN in autism [10,23,26,88–90]. Together they support the role for a common, sex-
489 independent DN role in autism. This is also supported by a recent autism neurosubtyping
490 study that identified three latent iFC factors, all sharing DN atypicalities along with their
491 neurosubtype-specific patterns [91]. Building on this evidence to disentangle the specific role
492 of each of the factors affecting autism in sex-independent and sex-dependent ways, a
493 necessary next step is to engage in novel large-scale data collection efforts including more
494 female data.
495
496 **Robustness, replicability and sources of variability**
497 The growing awareness of the replication crisis in neuroscience [92–94] motivated our
498 analyses examining robustness and replicability of findings. While a comprehensive and
499 systematic reproducibility assessment is beyond the scope of the study, here we focused on
500 examining whether the findings observed in the discovery analyses were also seen after using
501 different preprocessing pipelines – *robustness* – as well as in fully independent, albeit of
502 convenience samples (i.e., not harmonized *a priori* with each other) – *replicability*. To this
503 end, given the lack of consensus on quantitative metrics of replicability, we opted to use
504 measures of effect size. These are considered complementary to null hypothesis significance
505 testing [95]. In the context of this study, given the use of convenience samples of different
506 sizes, their selection was considered an advantageous and practical means to provide
507 information on the magnitude of group differences in diagnosis and sex, as well as their
508 interaction. Here, we considered findings to be robust and/or replicable for any non-
509 negligible effects (i.e., $\eta_p^2 \geq 0.01$; [69]). We reasoned that given their distributed and

heterogenous nature [6], atypicalities in the autism connectome can stem from a combination of differently sized non-negligible effects, as shown for autism in other biological domains such as genetics [96,97].

With this in mind, across the two preprocessing methods examined here, the patterns of findings were consistent with those observed in discovery analyses across all R-fMRI metrics and effects. These robustness results are consistent with a prior study by He and colleagues [46] reporting that differences in a wider range of pre-processing pipelines have marginal effects on variation in diagnostic group average comparisons. Our study confirms and builds on this earlier report by extending findings of robustness to sex group mean differences and their interactions with diagnosis.

A more nuanced picture emerged from the inter-sample analyses as replicability varied by sample, across the effects and R-fMRI metrics examined. Specifically, while inter-sample main effects of sex were moderately to largely replicable across R-fMRI metrics on both independent samples (~50 to 80% of the clusters in GENDAAR and EU-AIMS-LEAP, respectively), replicability of diagnostic effects significantly varied by sample (86% to 29%) across R-FMRI metrics. This is at least in part consistent with findings by King et al. [50] also showing that, depending on the R-fMRI feature examined, diagnostic group differences varied across samples. Even in this scenario, King et al. also reported that findings of decreased homotopic connectivity in autism were relatively more stable than other R-fMRI metrics [50]. This observation, combined with replicability of our VMHC sex-by-diagnosis interaction findings in the larger of the two independent samples (EU-AIMS LEAP), suggests that measures of homotopic connectivity may have a relevant biological relevance for autism.

534 It is also possible that given its moderate to high test-retest reliability, VMHC is more
535 suitable in efforts assessing replicability [98,99].
536
537 The striking clinical and biological heterogeneity in autism should be considered as a major
538 contributor to discrepancies in findings of studies focusing on the main effects of diagnostic
539 group means contrasts/interactions [100–103]. Against this background, we interpret our
540 replicability findings on diagnostic effects and, in turn, diagnosis-by-sex interactions. Inter-
541 sample differences may have contributed to the more variable results of replicability on the
542 diagnosis main effects. These may include autism symptom level, age, and IQ, albeit
543 secondary analyses suggested that the examined IQ range did not substantially affect the
544 pattern of discovery results. For example, the EU-AIMS LEAP sample was on-average older,
545 had lower VIQ and most notably, lower symptom severity across all subscales of the ADOS
546 and ADI-R than the ABIDE sample. On the other hand, the GENDAAR sample (which has
547 greater number of replicable diagnostic mean group patterns) did not differ from ABIDE in
548 these variables, except for mean age. Furthermore, a fact that is often neglected, is that the
549 NT groups may also present with considerable sample heterogeneity between studies
550 [100,104]. For instance, our NT controls in the EU-AIMS LEAP sample had lower VIQ than
551 both ABIDE and GENDAAR NT controls. This has potentially influenced the low
552 replicability of diagnosis main effects in EU-AIMS LEAP.
553
554 In contrast, sex-by-diagnosis effect on VMHC in the dorsolateral occipital cortex was
555 replicable in the larger samples, the EU-AIMS LEAP, but not in GENDAAR. Small samples
556 introduce larger epistemic variability (i.e., greater variation related to known and unknown
557 confounds) [105]. Increasing the number of subjects/data allows mitigating epistemic
558 variability and, thus, capturing the underlying variability of interest. Thus, although the rate

559 of EU-AIMS LEAP replicability for the main effect of diagnosis was limited, accounting for
560 biological sex, a known key source variability in autism, may have contributed to a replicable
561 sex-by-diagnosis pattern in this larger sample. In line with sample size concerns, using four
562 datasets sized between 36 and 44 individuals selected from the ABIDE repository, He et al.
563 [46] found low similarity rates of diagnostic group-level differences on the strength of iFC
564 edges in contrast with the largely similar pattern of results across pipelines. Of note, unlike
565 prior efforts [46,50], we controlled for site effects within each of the samples (i.e., ABIDE,
566 GENDAAR and EU-AIMS LEAP), using ComBat. Future large-scale harmonized data
567 collections are needed to control and assess the impact of inter-sample variability. Taken
568 together, these findings highlight that sample differences can impact replicability.
569
570 Beyond clinical and biological sources of variation, samples may differ in MRI acquisition
571 methods, as well as in approaches used to mitigate head motion during data collection and its
572 impact on findings [106]. Adequately controlling for head motion remains a key challenge for
573 future studies assessing inter-sample replicability. For the present study, we excluded
574 individuals with high motion, retained relatively large samples with group average low
575 motion (mean $\pm$ standard deviation range mFD range=0.09-0.16 $\pm$ 0.06-0.10 mm), as well as
576 included mFD at the second-level analyses as a nuisance covariate. Overall, the extent to
577 which each sample-related factor affects replicability needs to be systematically examined in
578 future well-powered studies. Only this type of studies will allow for emerging subtyping
579 approaches to dissect heterogeneity by brain imaging features using a range of data-driven
580 methods [107,108], including normative modelling [109–111].
581
582 Inter-sample differences and methodological differences, beyond nuisance regression, may
583 have contributed to some differences in findings between the present and earlier studies,

584 conducted with independent or partially overlapping samples [9,23,41]. For example, Alaerts
585 et al. [9] also examined sex-by-diagnosis interaction in PCC-iFC in a dataset selected from
586 ABIDE I only. Although their pattern of results was consistent with the 'gender incoherence'
587 model, the resulting circuit(s) did not involve the dorsolateral occipital cortex as identified
588 with VMHC in the present study. Along with differences in samples selected from the same
589 data repositories, other ABIDE-based methodological choices that may affect results. For
590 example, prior studies differed with the present one in the inclusion of sex-by-diagnosis
591 interaction [15], the extent of the whole-brain voxel-based analyses [13,14], or the statistical
592 threshold utilized [23]. Nevertheless, it is remarkable that even in light of these differences,
593 consistent results have emerged including the role of the 'gender incoherence' model for
594 females with autism, atypical inter-hemispheric interactions in autism, and sex-dependent and
595 sex-independent atypical intrinsic brain function across distinct functional networks.
596

597 ## Limitations

598 Along with the inter-sample differences resulting from the lack of sufficiently available
599 harmonized inter-site replication datasets in the field, other limitations of this study should be
600 addressed in future efforts. One regards the lack of measures differentiating the effects of sex
601 vs. that of gender so as to disentangle their relative roles (e.g., gender-identity and gender-
602 expression) in the intrinsic brain properties [112]. Further, in-depth cognitive measures to
603 directly characterize the role of VMHC findings were not available. Additional behavioral
604 measures are needed to establish whether our result in VMHC of the dorsolateral occipital
605 cortex mainly applies to low-level (bottom-up) visual processing differences or higher-level
606 (top-down) attentional/controlled processes in males and females with autism. As a
607 neurodevelopmental disorder, autism shows striking inter-individual differences in clinical
608 and developmental trajectories, as well as outcomes. Thus, age may influence symptom

presentation [113,114] and neurobiology [11,110,115]. Despite the considerable size of the samples available for this study, it is still difficult to sufficiently cover a broad age range across both males and females and diagnostic groups across contributing sites and to evaluate age effects appropriately. Even larger cross-sectional samples are needed to derive meaningful age-related information that ultimately require confirmation in longitudinal study designs. Such longitudinal studies would allow to examine the potential impact of puberty and related surge of sex steroids reported in NT boys and girls [116], in autism specifically. Here, we have no direct measure of puberty other than age, but future studies should aim to include such measures. Further, the value of a large-scale and publicly available multi-site resource such as ABIDE also comes with unavoidable differences in site differences which must be considered in data selection, analyses and interpretation of results. Although residual site-related effects may have remained in findings even after using the novel Bayesian approach for correcting for batch-effects, replicability in independent samples suggest that effects are not simply driven by site variability. These results are consistent with earlier reports of reproducible imaging biomarkers even when accounting for inter-site differences in multisite datasets such as the ABIDE I repository [47]. Finally, despite the advantages of effect sizes over p-value when comparing independently collected samples of different sizes and potentially different variances, it is important to acknowledge they are not without limitations [117] and should be interpreted with caution. Similar to p-values, they are dependent on sample sizes and have the equivalent risks of p-hacking. Finally, effect sizes standard errors can be large - a concern we addressed through including of confidence intervals.

Conclusions

633 The present work revealed sex differences in the intrinsic brain of autism, particularly in
634 dorsolateral occipital interhemispheric interactions, which were robust to pre-processing
635 pipeline decisions and replicable in the larger of the two independent samples. While
636 differences in nuisance regression pipelines have little influence on the consistency of
637 findings, sample heterogeneity represents a challenge for replicability of findings. Lateralized
638 cognitive functions and cross-hemispheric interactions should be further explored in relation
639 to sex differences in autism while addressing this challenge with future harmonized data
640 acquisition efforts with even larger samples.

641

642 **List of abbreviations**

643 ABIDE: Autism Brain Imaging Data Exchange

644 ASD: Autism spectrum disorder

645 DC: Degree centrality

646 DN: Default network

647 EPI: Echo-planar image

648 LEAP: Longitudinal European Autism Project

649 fALFF: Fractional amplitude of low frequency fluctuations

650 FIQ: Full-scale IQ

651 GENDAAR: Gender Explorations of Neurogenetics and Development to Advance Autism
652 Research

653 GSR: Global Signal Regression

654 ICA-AROMA: Independent Component Analysis - Automatic Removal of Motion Artifacts

655 iFC: Intrinsic functional connectivity

656 mFD: Mean framewise displacement

657 NDAR: National Database for Autism Research

NT: Neurotypical

PCC: Posterior cingulate cortex

ReHo: Regional Homogeneity

R-fMRI: Resting-state functional magnetic resonance imaging

VMHC: Voxel-mirrored homotopic connectivity

Ethics approval and consent to participate

ABIDE I and II: All contributions were based on studies approved by the local Institutional Review Boards, and data were fully anonymized (removing all 18 HIPAA (Health Insurance Portability and Accountability)-protected health information identifiers, and face information from structural images).

EU-AIMS LEAP: Ethical approval was obtained through ethics committees at each site.

GENDAAR: Informed assent and consent were obtained from all participants and their legal guardians, and the experimental protocol was approved by the Institutional Review Board at each participating site.

Consent for publication

Not applicable

Availability of data and materials

ABIDE I and II: Data are freely accessible in the publicly available Autism Brain Imaging Data Exchange repository (http://fcon_1000.projects.nitrc.org/indi/abide).

EU-AIMS LEAP: Data are currently only available for sites involved in data collection, but data (starting with the first wave) will be made available on request.

GENDAAR: Anonymized data are publicly available through the National Database for Autism Research (NDAR) and access can be requested via https://nda.nih.gov/about.html.

Competing interests

ADM receives royalties from the publication of the Italian version of the Social Responsiveness Scale—Child Version by Organization Speciali, Italy. JKB has been a consultant to, advisory board member of, and a speaker for Takeda/Shire, Medice, Roche, and Servier. He is not an employee of any of these companies and not a stock shareholder of any of these companies. He has no other financial or material support, including expert testimony, patents, or royalties. CFB is director and shareholder in SBGneuro Ltd. TC has received consultancy from Roche and Servier and received book royalties from Guildford Press and Sage. DM has been a consultant to, and advisory board member, for Roche and Servier. He is not an employee of any of these companies, and not a stock shareholder of any of these companies. TB served in an advisory or consultancy role for Lundbeck, Medice, Neurim Pharmaceuticals, Oberberg GmbH, Shire, and Infectopharm. He received conference support or speaker's fee by Lilly, Medice, and Shire. He received royalties from Hogrefe, Kohlhammer, CIP Medien, Oxford University Press; the present work is unrelated to these relationships. JT is a consultant to Roche. The remaining authors declare no competing interests.

Funding

Work for this study has been partly supported by a Postdoctoral Training Award from the Autism Science Foundation (to DLF/ADM); by NIMH (R21MH107045, R01MH105506, R01MH115363 to ADM); by gifts to the Child Mind Institute from Phyllis Green, Randolph Cowen, and Joseph Healey, and by UO1 MH099059 (to MPM); by the Ontario Brain

Institute via the Province of Ontario Neurodevelopmental Disorders Network (IDS-I l-02), the Slifka-Ritvo Award for Innovation in Autism Research from the International Society for Autism Research and the Alan B. Slifka Foundation, the Academic Scholars Award from the Department of Psychiatry, University of Toronto, the O'Brien Scholars Program in the Child and Youth Mental Health Collaborative at the Centre for Addiction and Mental Health (CAMH) and The Hospital for Sick Children, the Slaight Family Child and Youth Mental Health Innovation Fund from CAMH Foundation, and the Canadian Institutes of Health Research Sex and Gender Science Chair (GSB 171373) (to M-CL). We also acknowledge the contributions of all members of the EU-AIMS LEAP group. EU-AIMS LEAP has received funding from the Innovative Medicines Initiative 2 Joint Undertaking under grant agreement No 115300 (for EU-AIMS) and No 777394 (for AIMS-2-TRIALS). This joint undertaking receives support from the European Union's Horizon 2020 research and innovation program and EFPIA and AUTISM SPEAKS, Autistica, SFARI. DM is also supported by the NIHR Maudsley Biomedical Research Centre. SBC was supported by the Autism Research Trust during the period of this work.

Authors' contributions (in alphabetical order by contribution)

ADM and DLF have contributed to the study' s conception; ADM, DLF, JOAF, M-CL, MPM have contributed to distinct aspects of the study design and interpretation of all findings; DLF and JOAF conducted the analyses; SG has provided support in all data analyses requiring CPAC; ADM, DLF, JOAF have generated figures and tables; ADM and DLF drafted the manuscript; ADM, DLF, JOAF, M-CL, and MPM have revised and edited multiple versions of the manuscript; CFB, MM, MO, have organized the EU-AIMS LEAP data and edited latest manuscript versions and its revisions; CFB, CE, CM, DGMM, EL, FDA, GD, JKB, JT, SB-C, TC, TB, SD have contributed to the coordination, data acquisition and coordination of

732 the EU-AIMS LEAP project, as well as edited later versions of the manuscript and its
733 revisions. All authors read and approved the manuscript.
734

735 ## Acknowledgements

736 The authors thank all investigators and contributors to the Gender Explorations of
737 Neurogenetics and Development to Advance Autism Research (GENDAAR) for collecting
738 and sharing their data as well as addressing question related to the data, the Autism Brain
739 Imaging Data Exchange, and the contributors to EU-AIMS Longitudinal European Autism
740 Project for their efforts in data collection and sharing. The GENDAAR Consortium
741 comprises, in alphabetical order, Elizabeth H. Aylward, Raphael A. Bernier, Susan Y.
742 Bookheimer, Mirella Dapretto, Nadine Gaab, Daniel H. Geschwind, Andrei Irimia, Allison
743 Jack, Charles A. Nelson, Kevin A. Pelphrey, Matthew W. State, John D. Van Horn, Pamela
744 Ventola, and Sara J. Webb. We thank all participants and their families for participating in
745 the respective study.
746

747 ## References

748 1. Loomes R, Hull L, Mandy WPL. What Is the Male-to-Female Ratio in Autism Spectrum
749 Disorder? A Systematic Review and Meta-Analysis. J Am Acad Child Adolesc Psychiatry.
750 2017;56:466–74.
751 2. Floris DL, Lai MC, Nath T, Milham MP, Di Martino A. Network-specific sex
752 differentiation of intrinsic brain function in males with autism. Mol Autism. 2018;9.
753 3. Lai MC, Lombardo M V, Suckling J, Ruigrok ANV, Chakrabarti B, Ecker C, et al.
754 Biological sex affects the neurobiology of autism. Brain. 2013;136:2799–815.
755 4. Lai MC, Lerch JP, Floris DL, Ruigrok ANV, Pohl A, Lombardo M V., et al. Imaging
756 sex/gender and autism in the brain: Etiological implications. J Neurosci Res. Wiley-

Blackwell; 2017;95:380–97.

5. Ecker C. Notice of Retraction and Replacement: Ecker et al. Association between the probability of autism spectrum disorder and normative sex-related phenotypic diversity in brain structure. JAMA Psychiatry. 2017;74(4):329-338. JAMA Psychiatry. 2019. p. 549–50.

6. Picci G, Gotts SJ, Scherf KS. A theoretical rut: revisiting and critically evaluating the generalized under/over-connectivity hypothesis of autism. Dev Sci. 2016;19:524–49.

7. Geschwind DH, Levitt P. Autism spectrum disorders: developmental disconnection syndromes. Curr. Opin. Neurobiol. 2007. p. 103–11.

8. Smith REW, Avery JA, Wallace GL, Kenworthy L, Gotts SJ, Martin A. Sex Differences in Resting-State Functional Connectivity of the Cerebellum in Autism Spectrum Disorder. Front Hum Neurosci. 2019;13.

9. Alaerts K, Swinnen SP, Wenderoth N. Sex differences in autism: A resting-state fMRI investigation of functional brain connectivity in males and females. Soc Cogn Affect Neurosci. 2016;11:1002–16.

10. Ypma RJF, Moseley RL, Holt RJ, Rughooputh N, Floris DL, Chura LR, et al. Default Mode Hypoconnectivity Underlies a Sex-Related Autism Spectrum. Biol Psychiatry Cogn Neurosci Neuroimaging. 2016;1:364–71.

11. Kozhemiako N, Vakorin V, Nunes AS, Iarocci G, Ribary U, Doesburg SM. Extreme male developmental trajectories of homotopic brain connectivity in autism. Hum Brain Mapp. 2019;40:987–1000.

12. Lee JK, Amaral DG, Solomon M, Rogers SJ, Ozonoff S, Nordahl CW. Sex Differences in the Amygdala Resting-State Connectome of Children With Autism Spectrum Disorder. Biol Psychiatry Cogn Neurosci Neuroimaging. 2020;5:320–9.

13. Lawrence KE, Hernandez LM, Bowman HC, Padgaonkar NT, Fuster E, Jack A, et al. Sex Differences in Functional Connectivity of the Salience, Default Mode, and Central Executive

782 Networks in Youth with ASD. Cereb Cortex. 2020;30:5107–5120.

783 14. Hernandez LM, Lawrence KE, Padgaonkar NT, Inada M, Hoekstra JN, Lowe JK, et al.

784 Imaging-genetics of sex differences in ASD: distinct effects of OXTR variants on brain

785 connectivity. Transl Psychiatry. 2020;10.

786 15. Kozhemiako N, Nunes AS, Vakorin V, Iarocci G, Ribary U, Doesburg SM. Alterations in

787 Local Connectivity and Their Developmental Trajectories in Autism Spectrum Disorder:

788 Does Being Female Matter? Cereb Cortex. 2020;30:5166–79.

789 16. Olson LA, Mash LE, Linke A, Fong CH, Müller RA, Fishman I. Sex-related patterns of

790 intrinsic functional connectivity in children and adolescents with autism spectrum disorders.

791 Autism. 2020;24:2190–201.

792 17. Cummings KK, Lawrence KE, Hernandez LM, Wood ET, Bookheimer SY, Dapretto M,

793 et al. Sex Differences in Salience Network Connectivity and its Relationship to Sensory

794 Over-Responsivity in Youth with Autism Spectrum Disorder. Autism Res. 2020;13:1489–

795 500.

796 18. Henry TR, Dichter GS, Gates K. Age and Gender Effects on Intrinsic Connectivity in

797 Autism Using Functional Integration and Segregation. Biol Psychiatry Cogn Neurosci

798 Neuroimaging. 2018;3:414–22.

799 19. Baron-Cohen S. The extreme male brain theory of autism. Trends Cogn Sci. 2002;6:248–

800 54.

801 20. Bejerot S, Eriksson JM, Bonde S, Carlström K, Humble MB, Eriksson E. The extreme

802 male brain revisited: Gender coherence in adults with autism spectrum disorder. Br J

803 Psychiatry. 2012;201:116–23.

804 21. Watkins EE, Zimmermann ZJ, Poling A. The gender of participants in published research

805 involving people with autism spectrum disorders. Res Autism Spectr Disord. 2014;8:143–6.

806 22. Di Martino A, O'Connor D, Chen B, Alaerts K, Anderson JS, Assaf M, et al. Enhancing

807 studies of the connectome in autism using the autism brain imaging data exchange II. Sci
808 Data. 2017;4.
809 23. Di Martino A, Yan CG, Li Q, Denio E, Castellanos FX, Alaerts K, et al. The autism brain
810 imaging data exchange: Towards a large-scale evaluation of the intrinsic brain architecture in
811 autism. Mol Psychiatry. 2014;19:659–67.
812 24. Yan CG, Yang Z, Colcombe SJ, Zuo XN, Milham MP. Concordance among indices of
813 intrinsic brain function: Insights from inter-individual variation and temporal dynamics. Sci
814 Bull. 2017;62:1572–84.
815 25. Di Martino A, Fair DA, Kelly C, Satterthwaite TD, Castellanos FX, Thomason ME, et al.
816 Unraveling the miswired connectome: A developmental perspective. Neuron. 2014;83:1335–
817 53.
818 26. Assaf M, Jagannathan K, Calhoun VD, Miller L, Stevens MC, Sahl R, et al. Abnormal
819 functional connectivity of default mode sub-networks in autism spectrum disorder patients.
820 Neuroimage. 2010;53:247–56.
821 27. Lynch CJ, Uddin LQ, Supekar K, Khouzam A, Phillips J, Menon V. Default mode
822 network in childhood autism: Posteromedial cortex heterogeneity and relationship with social
823 deficits. Biol Psychiatry. 2013;74:212–9.
824 28. Lau WKW, Leung MK, Lau BWM. Resting-state abnormalities in Autism Spectrum
825 Disorders: A meta-analysis. Sci Rep. 2019;9.
826 29. Biswal BB, Mennes M, Zuo XN, Gohel S, Kelly C, Smith SM, et al. Toward discovery
827 science of human brain function. Proc Natl Acad Sci U S A. 2010;107:4734–9.
828 30. Dumais KM, Chernyak S, Nickerson LD, Janes AC. Sex differences in default mode and
829 dorsal attention network engagement. PLoS One. 2018;13.
830 31. Scheinost D, Finn ES, Tokoglu F, Shen X, Papademetris X, Hampson M, et al. Sex
831 differences in normal age trajectories of functional brain networks. Hum Brain Mapp.

2015;36:1524–35.

32. Yan CG, Craddock RC, Zuo XN, Zang YF, Milham MP. Standardizing the intrinsic brain: Towards robust measurement of inter-individual variation in 1000 functional connectomes. Neuroimage. 2013;80:246–62.

33. Zuo XN, Kelly C, Di Martino A, Mennes M, Margulies DS, Bangaru S, et al. Growing together and growing apart: Regional and sex differences in the lifespan developmental trajectories of functional homotopy. J Neurosci. 2010;30:15034–43.

34. Dinstein I, Pierce K, Eyler L, Solso S, Malach R, Behrmann M, et al. Disrupted Neural Synchronization in Toddlers with Autism. Neuron. 2011;70:1218–25.

35. Hahamy A, Behrmann M, Malach R. The idiosyncratic brain: Distortion of spontaneous connectivity patterns in autism spectrum disorder. Nat Neurosci. 2015;18:302–9.

36. Zang Y, Jiang T, Lu Y, He Y, Tian L. Regional homogeneity approach to fMRI data analysis. Neuroimage. 2004;22:394–400.

37. Paakki JJ, Rahko J, Long X, Moilanen I, Tervonen O, Nikkinen J, et al. Alterations in regional homogeneity of resting-state brain activity in autism spectrum disorders. Brain Res. 2010;1321:169–79.

38. Shukla DK, Keehn B, Müller RA. Regional homogeneity of fMRI time series in autism spectrum disorders. Neurosci Lett. 2010;476:46–51.

39. Zuo XN, Ehmke R, Mennes M, Imperati D, Castellanos FX, Sporns O, et al. Network centrality in the human functional connectome. Cereb Cortex. 2012;22:1862–75.

40. Di Martino A, Zuo XN, Kelly C, Grzadzinski R, Mennes M, Schvarcz A, et al. Shared and distinct intrinsic functional network centrality in autism and attention-deficit/hyperactivity disorder. Biol Psychiatry. 2013;74:623–32.

41. Holiga Š, Hipp JF, Chatham CH, Garces P, Spooren W, D'Ardhuy XL, et al. Patients with autism spectrum disorders display reproducible functional connectivity alterations. Sci

857 Transl Med. 2019;11.

858 42. Zou QH, Zhu CZ, Yang Y, Zuo XN, Long XY, Cao QJ, et al. An improved approach to

859 detection of amplitude of low-frequency fluctuation (ALFF) for resting-state fMRI:

860 Fractional ALFF. J Neurosci Methods. 2008;172:137–41.

861 43. Itahashi T, Yamada T, Watanabe H, Nakamura M, Ohta H, Kanai C, et al. Alterations of

862 local spontaneous brain activity and connectivity in adults with high-functioning autism

863 spectrum disorder. Mol Autism. 2015;6.

864 44. Ciric R, Wolf DH, Power JD, Roalf DR, Baum GL, Ruparel K, et al. Benchmarking of

865 participant-level confound regression strategies for the control of motion artifact in studies of

866 functional connectivity. Neuroimage. 2017;154:174–87.

867 45. Parkes L, Fulcher B, Yücel M, Fornito A. An evaluation of the efficacy, reliability, and

868 sensitivity of motion correction strategies for resting-state functional MRI. Neuroimage.

869 2018;171:415–36.

870 46. He Y, Byrge L, Kennedy DP. Nonreplication of functional connectivity differences in

871 autism spectrum disorder across multiple sites and denoising strategies. Hum Brain Mapp.

872 2020;41:1334–1350.

873 47. Abraham A, Milham MP, Di Martino A, Craddock RC, Samaras D, Thirion B, et al.

874 Deriving reproducible biomarkers from multi-site resting-state data: An Autism-based

875 example. Neuroimage. 2017;147:736–45.

876 48. Alaerts K, Nayar K, Kelly C, Raithel J, Milham MP, Di martino A. Age-related changes

877 in intrinsic function of the superior temporal sulcus in autism spectrum disorders. Soc Cogn

878 Affect Neurosci. 2015;10:1413–23.

879 49. Yahata N, Morimoto J, Hashimoto R, Lisi G, Shibata K, Kawakubo Y, et al. A small

880 number of abnormal brain connections predicts adult autism spectrum disorder. Nat

881 Commun. 2016;7.

882 50. King JB, Prigge MBD, King CK, Morgan J, Weathersby F, Fox JC, et al. Generalizability
883 and reproducibility of functional connectivity in autism. Mol Autism. 2019;10.
884 51. Charman T, Loth E, Tillmann J, Crawley D, Wooldridge C, Goyard D, et al. The EU-
885 AIMS Longitudinal European Autism Project (LEAP): Clinical characterisation. Mol Autism.
886 2017;8.
887 52. Loth E, Charman T, Mason L, Tillmann J, Jones EJH, Wooldridge C, et al. The EU-
888 AIMS Longitudinal European Autism Project (LEAP): Design and methodologies to identify
889 and validate stratification biomarkers for autism spectrum disorders. Mol Autism. 2017;8.
890 53. Irimia A, Torgerson CM, Jacokes ZJ, Van Horn JD. The connectomes of males and
891 females with autism spectrum disorder have significantly different white matter connectivity
892 densities. Sci Rep. 2017;7.
893 54. Jenkinson M, Bannister P, Brady M, Smith S. Improved optimization for the robust and
894 accurate linear registration and motion correction of brain images. Neuroimage.
895 2002;17:825–41.
896 55. Lefebvre A, Beggiato A, Bourgeron T, Toro R. Neuroanatomical Diversity of Corpus
897 Callosum and Brain Volume in Autism: Meta-analysis, Analysis of the Autism Brain
898 Imaging Data Exchange Project, and Simulation. Biol Psychiatry. 2015;78:126–34.
899 56. Dennis M, Francis DJ, Cirino PT, Schachar R, Barnes MA, Fletcher JMJM. Why IQ is
900 not a covariate in cognitive studies of neurodevelopmental disorders. J Int Neuropsychol Soc.
901 2009;15:331–43.
902 57. Friston KJ, Williams S, Howard R, Frackowiak RSJ, Turner R. Movement-related effects
903 in fMRI time-series. Magn Reson Med. 1996;35:346–55.
904 58. Behzadi Y, Restom K, Liau J, Liu TT. A component based noise correction method
905 (CompCor) for BOLD and perfusion based fMRI. Neuroimage. 2007;37:90–101.
906 59. Greve DN, Fischl B. Accurate and robust brain image alignment using boundary-based

907 registration. Neuroimage. 2009;48:63–72.

908 60. Avants BB, Tustison NJ, Wu J, Cook PA, Gee JC. An open source multivariate

909 framework for N-tissue segmentation with evaluation on public data. Neuroinformatics.

910 2011;9:381–400.

911 61. Nielson D, Pereira F, Zheng C, Migineishvili N, Lee J, Thomas A, et al. Detecting and

912 harmonizing scanner differences in the ABCD study - annual release 1.0. bioRxiv. 2018;

913 62. Eklund A, Nichols T. How open science revealed false positives in brain imaging.

914 Significance. 2017;14.

915 63. Thomas Yeo BT, Krienen FM, Eickhoff SB, Yaakub SN, Fox PT, Buckner RL, et al.

916 Functional specialization and flexibility in human association cortex. Cereb Cortex.

917 2015;25:3654–72.

918 64. Yarkoni T, Poldrack RA, Nichols TE, Van Essen DC, Wager TD. Large-scale automated

919 synthesis of human functional neuroimaging data. Nat Methods. 2011;8:665–70.

920 65. Gotham K, Pickles A, Lord C. Standardizing ADOS scores for a measure of severity in

921 autism spectrum disorders. J Autism Dev Disord. 2009;39:693–705.

922 66. Murphy K, Birn RM, Handwerker DA, Jones TB, Bandettini PA. The impact of global

923 signal regression on resting state correlations: Are anti-correlated networks introduced?

924 Neuroimage. 2009;44:893–905.

925 67. Pruim RHR, Mennes M, van Rooij D, Llera A, Buitelaar JK, Beckmann CF. ICA-

926 AROMA: A robust ICA-based strategy for removing motion artifacts from fMRI data.

927 Neuroimage. 2015;112:267–77.

928 68. Kong XZ, Consortium E, C F. An illustration of reproducibility in neuroscience research

929 in the absence of selective reporting. bioRxiv. 2020;

930 69. Cohen J. Statistical Power Analysis. Curr Dir Psychol Sci. 1992;1:98–101.

931 70. Hus V, Lord C. The autism diagnostic observation schedule, module 4: Revised algorithm

and standardized severity scores. J Autism Dev Disord. 2014;44:1996–2012.

71. Stark DE, Margulies DS, Shehzad ZE, Reiss P, Kelly AMC, Uddin LQ, et al. Regional variation in interhemispheric coordination of intrinsic hemodynamic fluctuations. J Neurosci. 2008;28:13754–64.

72. Floris DL, Howells H. Atypical structural and functional motor networks in autism. Prog Brain Res. 2018. p. 207–48.

73. Floris DL, Lai MC, Auer T, Lombardo M V., Ecker C, Chakrabarti B, et al. Atypically rightward cerebral asymmetry in male adults with autism stratifies individuals with and without language delay. Hum Brain Mapp. 2016;37:230–53.

74. Floris DL, Chura LR, Holt RJ, Suckling J, Bullmore ET, Baron-Cohen S, et al. Psychological correlates of handedness and corpus callosum asymmetry in autism: The left hemisphere dysfunction theory revisited. J Autism Dev Disord. 2013;43:1758–72.

75. Floris DL, Barber AD, Nebel MB, Martinelli M, Lai MC, Crocetti D, et al. Atypical lateralization of motor circuit functional connectivity in children with autism is associated with motor deficits. Mol Autism. 2016;7.

76. De Fossé L, Hodge SM, Makris N, Kennedy DN, Caviness VS, McGrath L, et al. Language-association cortex asymmetry in autism and specific language impairment. Ann Neurol. 2004;56:757–66.

77. Herbert MR, Ziegler D a, Deutsch CK, O'Brien LM, Kennedy DN, Filipek P a, et al. Brain asymmetries in autism and developmental language disorder: a nested whole-brain analysis. Brain. 2005;128:213–26.

78. Escalante-Mead PR, Minshew NJ, Sweeney JA. Abnormal brain lateralization in high-functioning autism. J Autism Dev Disord. 2003;33:539–43.

79. Flagg EJ, Cardy JEO, Roberts W, Roberts TPL. Language lateralization development in children with autism: insights from the late field magnetoencephalogram. Neurosci Lett.

957 2005;386:82–7.

958 80. Lindell AK, Hudry K. Atypicalities in cortical structure, handedness, and functional

959 lateralization for language in autism spectrum disorders. Neuropsychol Rev. 2013;23:257–70.

960 81. Floris DL, Wolfers T, Zabihi M, Holz NE, Zwiers MP, Charman T, et al. Atypical brain

961 asymmetry in autism – a candidate for clinically meaningful stratification. Biol Psychiatry

962 Cogn Neurosci Neuroimaging. 2020;

963 82. Zaidel E, Aboitiz F, Clarke J. Sexual dimorphism in interhemispheric relations:

964 Anatomical-behavioral convergence. Biol Res. 1995;28:27–43.

965 83. Proverbio AM, Brignone V, Matarazzo S, Del Zotto M, Zani A. Gender differences in

966 hemispheric asymmetry for face processing. BMC Neurosci. 2006;7.

967 84. Vogel JJ, Bowers CA, Vogel DS. Cerebral lateralization of spatial abilities: A meta-

968 analysis. Brain Cogn. 2003;52:197–204.

969 85. Kirkovski M, Enticott PG, Hughes ME, Rossell SL, Fitzgerald PB. Atypical Neural

970 Activity in Males But Not Females with Autism Spectrum Disorder. J Autism Dev Disord.

971 2016;46:954–63.

972 86. Lai MC, Lombardo M V., Chakrabarti B, Ruigrok ANV, Bullmore ET, Suckling J, et al.

973 Neural self-representation in autistic women and association with 'compensatory

974 camouflaging.' Autism. 2019;23:1210–23.

975 87. Lai MC, Lombardo M V., Auyeung B, Chakrabarti B, Baron-Cohen S. Sex/Gender

976 Differences and Autism: Setting the Scene for Future Research. J Am Acad Child Adolesc

977 Psychiatry. 2015;54:11–24.

978 88. Moseley RL, Ypma RJF, Holt RJ, Floris D, Chura LR, Spencer MD, et al. Whole-brain

979 functional hypoconnectivity as an endophenotype of autism in adolescents. NeuroImage Clin.

980 2015;9:140–52.

981 89. Kennedy DP, Courchesne E. Functional abnormalities of the default network during self-

and other-reflection in autism. Soc Cogn Affect Neurosci. 2008;3:177–90.

90. Hull J V., Jacokes ZJ, Torgerson CM, Irimia A, Van Horn JD, Aylward E, et al. Resting-state functional connectivity in autism spectrum disorders: A review. Front. Psychiatry. 2017.

91. Tang S, Sun N, Floris DL, Zhang X, Di Martino A, Yeo BTTT. Reconciling Dimensional and Categorical Models of Autism Heterogeneity: A Brain Connectomics and Behavioral Study. Biol Psychiatry. 2020;87:1071–82.

92. Barch DM, Yarkoni T. Introduction to the special issue on reliability and replication in cognitive and affective neuroscience research. Cogn Affect Behav Neurosci. 2013;13:687–9.

93. Poldrack RA, Poline JB. The publication and reproducibility challenges of shared data. Trends Cogn Sci. 2015;19:59–61.

94. Gorgolewski KJ, Nichols T, Kennedy DN, Poline JB, Poldrack RA. Making replication prestigious. Behav Brain Sci. 2018;41:e131.

95. Selya AS, Rose JS, Dierker LC, Hedeker D, Mermelstein RJ. A practical guide to calculating Cohen's f 2, a measure of local effect size, from PROC MIXED. Front Psychol. 2012;3.

96. Gratten J, Wray NR, Keller MC, Visscher PM. Large-scale genomics unveils the genetic architecture of psychiatric disorders. Nat Neurosci. 2014;17:782–90.

97. Sanders SJ, He X, Willsey AJ, Ercan-Sencicek AG, Samocha KE, Cicek AE, et al. Insights into Autism Spectrum Disorder Genomic Architecture and Biology from 71 Risk Loci. Neuron. 2015;87:1215–33.

98. Zuo XN, Xing XX. Test-retest reliabilities of resting-state FMRI measurements in human brain functional connectomics: A systems neuroscience perspective. Neurosci Biobehav Rev. 2014;45:100–18.

99. Zuo XN, Xu T, Milham MP. Harnessing reliability for neuroscience research. Nat Hum Behav. 2019;3:768–71.

1007 100. Feczko E, Miranda-Dominguez O, Marr M, Graham A, Nigg J, Fair D. The
1008 Heterogeneity Problem: Approaches to Identify Psychiatric Subtypes. Trends Cogn Sci.
1009 2019;23:584–601.
1010 101. Marquand AF, Wolfers T, Mennes M, Buitelaar J, Beckmann CF. Beyond Lumping and
1011 Splitting: A Review of Computational Approaches for Stratifying Psychiatric Disorders. Biol
1012 Psychiatry Cogn Neurosci Neuroimaging. 2016;1:433–47.
1013 102. Lombardo M V., Lai MC, Baron-Cohen S. Big data approaches to decomposing
1014 heterogeneity across the autism spectrum. Mol Psychiatry. 2019;24:1435–50.
1015 103. Wolfers T, Floris DL, Dinga R, van Rooij D, Isakoglou C, Kia SM, et al. From pattern
1016 classification to stratification: towards conceptualizing the heterogeneity of Autism Spectrum
1017 Disorder. Neurosci Biobehav Rev. 2019;104:240–54.
1018 104. Yokota S, Takeuchi H, Hashimoto T, Hashizume H, Asano K, Asano M, et al.
1019 Individual differences in cognitive performance and brain structure in typically developing
1020 children. Dev Cogn Neurosci. 2015;14:1–7.
1021 105. Marquand AF, Kia SM, Zabihi M, Wolfers T, Buitelaar JK, Beckmann CF.
1022 Conceptualizing mental disorders as deviations from normative functioning. Mol Psychiatry.
1023 2019;24:1415–1424.
1024 106. van Dijk KRA, Sabuncu MR, Buckner RL. The influence of head motion on intrinsic
1025 functional connectivity MRI. Neuroimage. 2012;59:431–8.
1026 107. Hong S-J, Vogelstein JT, Gozzi A, Bernhardt BC, Yeo BTT, Milham MP, et al.
1027 Towards Neurosubtypes in Autism. Biol Psychiatry. 2020;88:111–28.
1028 108. Zabihi M, Floris DL, Kia SM, Wolfers T, Tillmann J, Arenas AL, et al. Fractionating
1029 autism based on neuroanatomical normative modeling. Transl Psychiatry. 2020;10.
1030 109. Marquand AF, Rezek I, Buitelaar J, Beckmann CF. Understanding Heterogeneity in
1031 Clinical Cohorts Using Normative Models: Beyond Case-Control Studies. Biol Psychiatry.

2016;80:552–61.

110. Zabihi M, Oldehinkel M, Wolfers T, Frouin V, Goyard D, Loth E, et al. Dissecting the Heterogeneous Cortical Anatomy of Autism Spectrum Disorder Using Normative Models. Biol Psychiatry Cogn Neurosci Neuroimaging. 2019;4:567–78.

111. Floris DL, Wolfer T, Zabihi M, Holz N, Zwiers M, Charman T, et al. Atypical brain asymmetry in autism - a candidate for clinically meaningful stratification. BioRxiv. 2020;

112. Strang JF, van der Miesen AI, Caplan R, Hughes C, DaVanport S, Lai M-C. Both sex- and gender-related factors should be considered in autism research and clinical practice. Autism. 2020;24:539–43.

113. Charman T, Taylor E, Drew A, Cockerill H, Brown JA, Baird G. Outcome at 7 years of children diagnosed with autism at age 2: Predictive validity of assessments conducted at 2 and 3 years of age and pattern of symptom change over time. J Child Psychol Psychiatry Allied Discip. 2005;46:500–13.

114. Fecteau S, Mottron L, Berthiaume C, Burack JA. Developmental changes of autistic symptoms. Autism. 2003;7:255–68.

115. Lin HY, Ni HC, Lai MC, Tseng WYI, Gau SSF. Regional brain volume differences between males with and without autism spectrum disorder are highly age-dependent. Mol Autism. 2015;6.

116. Peper JS, Brouwer RM, Schnack HG, van Baal GC, van Leeuwen M, van den Berg SM, et al. Sex steroids and brain structure in pubertal boys and girls. Psychoneuroendocrinology. 2009;34.

117. Maher JM, Markey JC, Ebert-May D. The other half of the story: Effect size analysis in quantitative research. CBE Life Sci Educ. 2013;12.

Figure Captions

Fig 1. Overlap across R-fMRI metrics for main effects of diagnosis and sex

Upper panel: the surface inflated maps depict the extent of overlap across clusters showing significant main effects of diagnosis (left) and sex (right) across any of three resting state fMRI (R-fMRI) metrics showing statistically significant effects ($Z > 3.1$, $P<0.01$). Purple clusters represent areas of significant group differences emerging for only one of any of the three R-fMRI measures, orange and yellow clusters indicate measures with overlap among 2 and 3 R-fMRI measures (see Additional file 5 for statistical maps of main effects for each R-fMRI metric). Cluster masks are overlaid on inflated brain maps generated by BrainNet Viewer. Lower panel: for each of the yellow and orange clusters in panel A, the table lists the cluster's anatomical label based on the Harvard Oxford atlas, the specific R-fMRI metrics involved, and the group difference direction (ASD<NT or M<F in blue, ASD>NT or M>F in red). Abbreviations**:** L= Left hemisphere; R= Right hemisphere, PCG/FP=Paracingulate cortex/frontal pole, ACC=Anterior cingulate cortex, PCC/Prec=Posterior cingulate cortex/precuneus, ASD=autism spectrum disorder, NT=neurotypical, M=Males, F=Females).

Fig 2. Sex-by-diagnosis interaction effect, its robustness and replicability

a) On the right, surface maps show the cluster with a significant ($Z > 3.1$, $P<0.01$) sex-by-diagnosis interaction for voxel-mirrored homotopic connectivity (VMHC) resulting from discovery analyses in the ABIDE sample using the component-based noise reduction (CompCor) pipeline. The statistical Z maps are overlaid on inflated brain maps generated by BrainNet Viewer. b) The upper panels show the pattern of VMHC group means in males and females by each diagnostic group (ASD and NT) extracted from the same cluster in data pre-processed following two alternative denoising pipelines, Global Signal Regression (GSR,

left) and Independent Component Analysis – Automatic Removal of Motion Artifacts (ICA-AROMA, right). Results show a pattern similar to the those observed in discovery analyses with small to moderate effect sizes (η_p^2range=0.01–0.07). c) The lower graph shows replicability in two independent samples: the Gender Explorations of Neurogenetics and Development to Advance Autism Research (GENDAAR) and the EU-AIMS Longitudinal European Autism Project (LEAP). The pattern of results was replicable in the EU-AIMS LEAP (N=309) with a small effect size (η_p^2= 0.01) and had a negligible effect size in GENDAAR sample (N=196; η_p^2< 0.01). For all graphs VMHC data are shown as residuals obtained after regressing out mean framewise displacement and age effects. Abbreviations: L=left, R=right, A=anterior, P=posterior.

Fig 3. Functional relevance of sex-by-diagnosis interaction in VMHC

a) The radar plot shows the percentage (0-80%) of overlap between the voxels in the dorsolateral occipital cluster showing a significant VMHC sex-by-diagnosis interaction in discovery analyses and the 12 Yeo cognitive ontology probability maps [63] (probability threshold at *P* = 1e-5) for cognitive components C1-C12. As in Floris et al. [2], we labelled each component based on the top five tasks reported to be most likely recruited by a given component. b) Word cloud based on the top 27 terms showing correlations between *r*=0.64 to *r*=0.10 associated with the same VMHC cluster based on the Neurosynth Image Decoder. c) Sex-differential association between each individual's VMHC at the cluster showing a significant sex-by-diagnosis interaction in primary analyses and available ADOS social-affect uncalibrated sub-scores in males and females with ASD. VMHC data are shown as residuals obtained after regressing out mean framewise displacement and age effects. While males showed no significant associations at corrected and uncorrected thresholds, females with

lower dorsolateral occipital VMHC showed more severe social-affect symptoms at uncorrected statistical threshold ($F_{(1,311)}$=4.44, p=0.036).

Fig 4. Robustness and replicability summary

a) The histogram summarizes the percentage of clusters showing a robust and replicable pattern of results as that observed in discovery analyses in the ABIDE sample for main effects of diagnosis (Dx; green; N=7 clusters), sex (yellow; N=10 clusters) and their interaction (blue; N=1 cluster) across three R-fMRI metrics. All findings were robust to different preprocessing pipelines. Across R-fMRI metrics, main sex effects were moderately (50%) to largely (80%) replicable across independent samples: Gender Explorations of Neurogenetics and Development to Advance Autism Research (GENDAAR) and the EU-AIMS Longitudinal European Autism Project (LEAP), respectively. Replicability for main effects of diagnosis was largely replicable in GENDAAR (86%) and minimally replicable in EU-AIMS LEAP (29%). The VMHC pattern observed for sex-by-diagnosis interaction in primary discovery analyses was replicated in EU-AIMS LEAP only. b) Surface conjunction maps show the clusters replicated in GENDAAR only (G, purple), EU-AIMS LEAP only (E, blue) and in both samples (G&E, red) for each effect separately. Cluster masks are overlaid on inflated brain maps generated by BrainNet Viewer.

Additional files

Additional file 1

Title: Supplementary Material

File format: docx

Description: Supplementary Methods

Additional file 2

Title: Selection flowchart for the ABIDE sample

File format: tif

Description: The flowchart illustrates the selection process resulting in the final ABIDE I and II combined sample of 1019 subjects. At each flowchart step, the numbers outside the parentheses represent the total number of datasets across both ABIDE I and ABIDE II; in parenthesis are the number of datasets derived from ABIDE I (the resulting difference between these numbers would be the numbers for dataset stemming from ABIDE II). The rationale for each selection step is detailed in Supplementary Material. Abbreviations: ASD=autism spectrum disorder, NT=neurotypical, A I=ABIDE I.

Additional file 3

Title: Supplementary Tables

File format: docx

Description: Characterization of EU-AIMS LEAP and GENDAAR samples, comparison between samples and summary table of main effects.

Additional file 4

Title: Main effects of diagnosis and sex in the ABIDE discovery sample

File format: tif

Description: Significant results (Z >3.1, P<0.01, corrected) of voxel-wise discovery analyses conducted in the ABIDE dataset for main effects (ME) of diagnosis (left) and sex (right) for seed-based intrinsic functional connectivity of the posterior cingulate cortex- (PCC), voxel mirror homotopic connectivity (VMHC), and Regional Homogeneity (ReHo). Significant clusters are overlaid on inflated brain maps generated by BrainNet Viewer. No significant effects were detected for degree centrality or fractional amplitude of low frequency fluctuations. ME Diagnosis: PCC-iFC: bilateral paracingulate cortex and frontal pole

(PCG/FP), superior lateral occipital cortex (sLOC), temporal occipital fusiform cortex and occipital fusiform gyrus (TOFC/OFC); VMHC: bilateral posterior cingulate gyrus and precuneus (PCC/Prec), PCG/FP; ReHo: PCG/FP, central operculum and insula (CO/Ins). ME Sex: PCC-iFC: bilateral sLOC, middle frontal gyrus (MFG), bilateral PCC/Prec, bilateral PCG/FP; VMHC: bilateral PCC/Prec, bilateral anterior cingulate cortex (ACC); ReHo: bilateral PCC, angular gyrus and lateral occipital cortex (AnG/LOC). See Additional file 3: Table S6 for details on each cluster sizes. *Due to processing failure of two subjects for VMHC, the sample size comprised 1017 subjects instead of 1019.

Additional file 5

Title: Characteristics of the clusters with significant effect and effect size across analyses

File format: pdf

Description: Additional file 5 summarizes cluster' anatomical labels, center of gravity coordinates and statistics derived from discovery analyses, as well as effect size and their confidence of interval for each of these clusters across all analyses In green are the effect found to be robust/replicable based on our criteria (*i.e.*, the group mean difference(s) in the same direction as those identified in discovery analyses and effect sizes not negligible as defined by partial eta squared η_p^2 <0.01) and in yellow those that did not. PCC-iFC: posterior cingulate cortex intrinsic functional connectivity, VMHC: voxel-mirrored homotopic connectivity, ReHo: regional homogeneity, TOFC/OFG: temporal occiptal fusiform cortex/occiptal fusiform gyrus, sLOC: superior lateral occipital cortex, PCG/FP: paracingulate cortex/frontal pole, PCC/Prec: posterior cingulate gyrus/precuneus, CO/Ins: central operculum/insula, MFG: middle frontal gyrus, ACC: anterior cingulate cortex, SMG: supramarginal gyrus, AnG/LOC: angular gyrus/lateral occipital cortex. *Due to processing

failure of two subjects for VMHC, the sample size comprised 1017 subjects instead of 1019 for ABIDE and 307 instead of 309 for EU-AIMS.

Additional file 6

Title: Main effects of diagnosis and sex in the ABIDE discovery sample when additionally covarying for FIQ

File format: tif

Description: Including full-scale IQ (FIQ) as a nuisance regressor in addition to age and mean FD in the voxel-wise model yielded significant (Z>3.1, P<0.01, corrected) findings highly similar to those observed in discovery analyses across main effects (ME) of diagnosis (left) and sex (right), sex and their interaction. As in the discovery approach, analyses were conducted for seed-based intrinsic functional connectivity of the posterior cingulate cortex- (iFC-PCC), voxel mirror homotopic connectivity (VMHC), and Regional Homogeneity (ReHo). Significant clusters are overlaid on inflated brain maps generated by BrainNet Viewer. No significant effects were detected for degree centrality or fractional amplitude of low frequency fluctuations. ME Diagnosis: PCC-iFC: bilateral paracingulate cortex and frontal pole (PCG/FP), superior lateral occipital cortex (sLOC), temporal occipital fusiform cortex and occipital fusiform gyrus (TOFC/OFC); VMHC: bilateral posterior cingulate gyrus and precuneus (PCC/Prec), PCG/FP; ReHo: PCG/FP, central operculum and insula (CO/Ins). ME Sex: PCC-iFC: bilateral sLOC, middle frontal gyrus (MFG), bilateral PCC/Prec, bilateral PCG/FP; VMHC: bilateral PCC/Prec, bilateral anterior cingulate cortex (ACC); ReHo: bilateral PCC, angular gyrus and lateral occipital cortex (AnG/LOC). Sex-by-diagnosis: VMHC: bilateral dorsolateral occipital cortex. *Due to processing failure of two subjects for VMHC, the sample size comprised 1017 subjects instead of 1019.

Additional file 7

Title: Stability of main effects

File format: tif

Description: Inter-site stability was assessed after extracting group means at masks corresponding to the clusters showing significant main effects of diagnosis (7a) and sex (7b) in the discovery analyses and then deriving the group mean when leaving one acquisition site out at the time. The pattern of results was unchanged. Different ABIDE sites are color-coded on legend on the side. Due to processing failure of two subjects for VMHC, the sample size comprised 1017 subjects. Abbreviations: ASD=autism spectrum disorder, NT=neurotypical, PCC-iFC=posterior cingulate cortex intrinsic functional connectivity (x=0, y=-53, z=26), VMHC=voxel-mirrored homotopic connectivity, ReHo=regional homogeneity, L=left, R=right. Different sites in ABIDE are color-coded on the top left. Data are shown as residuals obtained after regressing out mean framewise displacement and age effects.

Additional file 8

Title: Stability of sex-by-diagnosis interaction effect

File format: tif

Description: Inter-site stability of the sex-by-diagnosis interaction pattern was assessed after extracting group means at the mask corresponding to the clusters showing a significant interaction in the discovery analyses and then deriving the group mean when leaving one acquisition site out at the time. The pattern of results was unchanged. Different sites in ABIDE are color-coded in the legend on the right. Due to processing failure of two subjects for VMHC, the sample size comprised 1017 subjects. Abbreviations: ASD=autism spectrum disorder, NT=neurotypical, PCC-iFC=posterior cingulate cortex intrinsic functional connectivity (x=0, y=-53, z=26), VMHC=voxel-mirrored homotopic connectivity,

ReHo=regional homogeneity, L=left, R=right. Different sites in ABIDE are color-coded on the top left.

Additional file 9

Title: Robustness to nuisance corrections of main effects of diagnosis and sex

File format: tif

Description: Cluster-level replication of the results emerging from the voxel-wise discovery analyses in the ABIDE dataset preprocessed using CompCor for the statistically significant main effects of diagnosis (9a) and sex (9b) after preprocessing with GSR and with ICA-AROMA. The second column on the left shows the clusters (Z>3.1, P<0.01, corrected) with significant diagnostic and sex effects for posterior cingulate cortex intrinsic functional connectivity (PCC-iFC), voxel-mirrored homotopic connectivity (VMHC), and regional homogeneity (ReHo). Results are overlaid on inflated brain maps generated by BrainNet Viewer. The bar plots represent the residual means resulting from regressing out diagnosis or sex effects depending on the desired main effect from the cluster means. 9a) The ABIDE GSR and ABIDE ICA-AROMA columns illustrate, for each of these R-fMRI indices, the diagnostic group mean pattern across clusters with a diagnostic effect size of $\eta_p^2 \geq 0.01$. Color codes: Red=ASD; Green=NT. PCC-iFC: bilateral paracingulate cortex and frontal pole (PCG/FP), superior lateral occipital cortex (sLOC), temporal occipital fusiform cortex and occipital fusiform gyrus (TOFC/OFC); VMHC: bilateral posterior cingulate gyrus and precuneus (PCC/Prec), PCG/FP; ReHo: PCG/FP, central operculum and insula (CO/Ins). ABIDE GSR: 7 out of 7 main effects of diagnosis replicated (100%). ABIDE ICA-AROMA: 7 out of 7 main effects of diagnosis replicated (100%) 9b) The ABIDE GSR and ABIDE ICA-AROMA columns illustrate, for each of these R-fMRI indices, the sex group mean pattern across clusters with an effect size of $\eta_p^2 \geq 0.01$. Color codes: Blue=males; Pink=females. PCC-iFC: bilateral sLOC, middle frontal gyrus (MFG), bilateral PCC/Prec,

bilateral PCG/FP; VMHC: bilateral PCC/Prec, bilateral anterior cingulate cortex (ACC); ReHo: bilateral PCC, angular gyrus and lateral occipital cortex (AnG/LOC). ABIDE GSR: 10 out of 10 main effects of diagnosis replicated (100%). ABIDE ICA-AROMA: 10 out of 10 main effects of diagnosis replicated (100%). Due to processing failure of two subjects for VMHC, the sample size comprised 1017 subjects instead of 1019. VMHC data are shown as residuals obtained after regressing out mean framewise displacement and age effects. Abbreviations: ASD=autism spectrum disorder, NT=neurotypical, M=males, F=females, CompCor=component base noise reduction, GSR=Global Signal Regression, ICA-AROMA=independent component analysis – automatic removal of motion artifacts, PCC-iFC=posterior cingulate cortex intrinsic functional connectivity (x=0, y=-53, z=26), VMHC=voxel-mirrored homotopic connectivity, ReHo=regional homogeneity, L=left, R=right, R+=replication based on same direction of results and $\eta_p^2 \geq 0.01$, R-=non-replication of results (displayed in gray plots).

Additional file 10

Title: Replicability of main effects of diagnosis and sex

File format: tif

Description: Cluster-level replication of the results emerging from the voxel-wise analyses in the ABIDE dataset for main effects of diagnosis (10a) and sex (10b) in the Gender Explorations of Neurogenetics and Development to Advance Autism Research (GENDAAR) and the EU-AIMS Longitudinal European Autism Project (LEAP) samples. The ABIDE column on the left shows the clusters ($Z>3.1$, $P<0.01$, corrected) with significant diagnostic and sex effects for posterior cingulate cortex intrinsic functional connectivity (PCC-iFC), voxel-mirrored homotopic connectivity (VMHC), and regional homogeneity (ReHo). No significant effects were detected for degree centrality and fractional amplitude of low frequency fluctuations. Results are overlaid on inflated brain maps generated by BrainNet

Viewer. The bar plots represent the residual means resulting from the linear Gaussian regression for each group. 10a**)** The GENDAAR and EU-AIMS LEAP columns illustrate, for each R-fMRI index, the diagnostic group mean pattern across clusters with a diagnostic effect size of $\eta_p^2 \geq 0.01$. Color codes: Red=ASD; Green=NT. PCC-iFC: bilateral paracingulate cortex and frontal pole (PCG/FP), superior lateral occipital cortex (sLOC), temporal occipital fusiform cortex and occipital fusiform gyrus (TOFC/OFC); VMHC: bilateral posterior cingulate gyrus and precuneus (PCC/Prec), PCG/FP; ReHo: PCG/FP, central operculum and insula (CO/Ins). GENDAAR: 6 out of 7 main effects of diagnosis replicated (86%); EU-AIMS LEAP: 2 out of 7 main effects of diagnosis replicated (29%). 10b**)** The GENDAAR and EU-AIMS LEAP columns illustrate, for each of these R-fMRI index, the sex group mean pattern across clusters with an effect size of $\eta_p^2 \geq 0.01$. Color codes: Blue=males, Pink=females. PCC-iFC: bilateral sLOC, middle frontal gyrus (MFG), bilateral PCC/Prec, bilateral PCG/FP; VMHC: bilateral PCC/Prec, bilateral anterior cingulate cortex (ACC); ReHo: bilateral PCC, angular gyrus and lateral occipital cortex (AnG/LOC). GENDAAR: 5 out of 10 main effects of sex replicated (50%); EU-AIMS LEAP: 8 out of 10 main effects of sex replicated (80%). *Due to processing failure of two subjects for VMHC, the sample size comprised 1017 subjects instead of 1019. Abbreviations: ASD=autism spectrum disorder, NT=neurotypical, M=males, F=females, PCC-iFC=posterior cingulate cortex intrinsic functional connectivity (x=0, y=-53, z=26), VMHC=voxel-mirrored homotopic connectivity, ReHo=regional homogeneity, L=left, R=right, R+=replication based on same direction of results and $\eta_p^2 \geq 0.01$, R-=non-replication of results.

1291 **Table 1. Characterization of sample merged across ABIDE I and II**

ABIDE I + II	Sites[a]	ASD M (N=362)	ASD F (N=82)	NT M (N=409)	NT F (N=166)		
	N	**Mean (SD) [Range]**	**Mean (SD) [Range]**	**Mean (SD) [Range]**	**Mean (SD) [Range]**	**Statistics**	**Post-hoc**
Age	13	11.8 (2.6) [7-17.9]	11.7 (2.7) [7-18]	11.8 (2.6) [7.1-18.2]	11.4 (2.3) [7.8-17.4]	$F_{(3)}$=1.18, p=0.32	
Full-Scale IQ[b]	13	106 (16.6) [72-148]	104 (16.3) [73-147]	112 (12.7) [73-148]	114 (12.7) [80-144]	$F_{(3)}$=19.24, p<0.001	(ASD M=ASD F) < (NT M=NT F)
Verbal IQ[c]	12	107 (17.9) [57-180]	105 (17.3) [62-145]	114 (13.5) [73-147]	114 (14.4) [83-146]	$F_{(3)}$=16.78, p<0.001	(ASD M=ASD F) < (NT M=NT F)
Performance IQ[d]	12	106 (17.0) [59-157]	104 (17.1) [67-148]	109 (14.2) [62-147]	109 (13.2) [79-145]	$F_{(3)}$=3.1, p=0.03	(ASD M=ASD F) < (NT M=NT F)
Mean FD	13	0.11 (0.07) [0.02-0.39]	0.13 (0.09) [0.02-0.39]	0.09 (0.06) [0.02-0.39]	0.09 (0.06) [0.02-0.38]	$H_{(3)}$=29.6, p<0.001	(ASD M=ASD F) < (NT M=NT F)
ADI-R							
Social[e]	11	19.7 (5.2) [4-30]	19.6 (5.5) [7-30]	-	-	$t_{(93)}$=0.14, p=0.89	
Communication[f]	11	15.6 (4.5) [2-25]	15.2 (5.0) [4-24]	-	-	$t_{(92)}$=0.61, p=0.54	
RRB[f]	11	6.0 (2.4) [0-13]	5.8 (2.5) [0-12]	-	-	$t_{(96)}$=0.51, p=0.61	
ADOS-2							
Social-Affect[g]	11	9.1 (3.7) [1-20]	8.7 (3.2) [4-18]	-	-	$t_{(87)}$=0.97, p=0.33	
RRB[h]	11	3.2 (1.8) [0-8]	2.8 (1.5) [0-5]	-	-	$t_{(93)}$=1.79, p=0.08	
CSS total[i]	11	6.9 (2.1) [1-10]	6.8 (1.8) [2-10]	-	-	$t_{(93)}$=0.11, p=0.32	
		N	**N**			**Statistics**	**Post-hoc**

Comorbidity	5	99[j]	25[h]	-	-	$\chi^2_{(1)}$=0.2, p=0.66
Psychoactive Meds	10	112	26	-	-	$\chi^2_{(1)}$<0.01, p=0.99

Abbreviations: *ABIDE*: Autism Brain Imaging data exchange; *ADI-R* = Autism Diagnostic Interview-Revised; *ADOS-2* = Autism Diagnostic Observation Schedule-2; *ASD* = Autism Spectrum Disorder; *CSS* = Calibrated Severity Score*; F* = females; *IQ* = intellectual quotient; *M* = males; *Mean FD* = mean framewise displacement [54]; *NT* = neurotypical; RRB= restricted repetitive behaviors. **Notes**: [a]ABIDE I data collections: KKI, Leuven_2, NYU, OHSU, Pitt, SDSU, Stanford, UCLA_1, UM_1, and Yale. ABIDE II data collections: ABIDEII-GU_1, ABIDEII-KKI_1, ABIDEII-KKI_2, ABIDEII-NYU_1, ABIDEII-OHSU_1, ABIDEII-SDSU_1, ABIDEII-UCD_1 and ABIDEII-UCLA_1. KKI and ABIDEII-KKI_1, NYU and ABIDEII-NYU_1, SDSU and ABIDEII-SDSU_1, OHSU and ABIDEII-OHSU_1 and UCLA_1 and ABIDEII-UCLA_1 were merged into one site across ABIDE I and ABIDE II collections. [b]FIQ was available for 362 males with ASD (2 missing from UM_1, ABIDEII-SDSU_1), 81 females with ASD (1 missing from ABIDEII-GU_1), 407 neurotypical males (NT M) (3 missing from ABIDEII-GU_1 (N=1), UM_1 (N=2)) and all 166 NT females (NT F). [c]VIQ was available for 315 males with ASD (47 missing; KKI (N=14), ABIDEII-OHSU_1 (N=22), OHSU (N=9), ABIDEII-SDSU_1 (N=1); ABIDEII-UCLA_1 (N=1), 70 females with ASD (12 missing, ABIDEII-GU_1 (N=1), KKI (N=4), ABIDEII-OHSU_1 (N=7)), 351 NT M (59 missing; ABIDEII-GU_1 (N=1), KKI (N=23), OHSU (N=15), ABIDEII-OHSU_1 (N=20)), and 139 NT F (27 missing; KKI (N=8), ABIDEII-OHSU_1 (N=19)). [d]PIQ was available for 306 males with ASD (56 missing; ABIDEII-GU_1 (N=9), KKI (N=14), OHSU (N=9), ABIDEII-OHSU_1 (N=22), ABIDEII-UCLA_1 (N=1), UM_1, (N=1)), 67 females with ASD (15 missing; ABIDEII-GU_1 (N=4), KKI (N=4), ABIDEII-OHSU_1 (N=7)), 349 NT M (61 missing; ABIDEII-GU_1 (N=1), KKI (N=23), OHSU (N=15), ABIDEII-OHSU_1 (N=20), UM_1, (N=2)), 139 NT F (27 missing; KKI (N=8), ABIDEII-OHSU_1 (N=19)). [e]ADI-R Social scores were available for 317 males with ASD (45 missing; ABIDEII-GU_1 (N=1), Leuven_2 (N=10), NYU (N=3), ABIDEII-NYU_1 (N=1), SDSU (N=2), ABIDEII-UCD_1 (N=11), ABIDEII-UCLA_1 (N=14), UM_1, (N=2), Yale (N=3)) and 68 females with ASD (14 missing; ABIDEII-GU_1 (N=1), ABIDEII-KKI_1 (N=2), Leuven_2 (N=3), NYU (N=1), Pitt (N=1), ABIDEII-UCD_1 (N=3), ABIDEII-UCLA_1 (N=1), Yale (N=2)). [f]ADI-R Communication and RRB scores were

available for 318 males with ASD (45 missing; ABIDEII-GU_1 (N=1), Leuven_2 (N=10), NYU (N=2), ABIDEII-NYU_1 (N=1), SDSU (N=2), ABIDEII-UCD_1 (N=11), ABIDEII-UCLA_1 (N=14), UM_1, (N=2), Yale (N=3)) and 68 females with ASD (14 missing; ABIDEII-GU_1 (N=1), ABIDEII-KKI_1 (N=2), Leuven_2 (N=3), NYU (N=1), Pitt (N=1), ABIDEII-UCD_1 (N=3), ABIDEII-UCLA_1 (N=1), Yale (N=2)). [g]ADOS-Gotham Social-Affect was available for 261 males with ASD (101 missing; ABIDEII-GU_1 (N=27), ABIDEII-KKI_1 (N=13), Leuven_2 (N=10), NYU (N=7), OHSU (N=11), Pitt (N=8), SDSU (N=8), Stanford (N=6), ABIDEII-UCLA_1 (N=5), UM_1 (N=6), Yale (N=1)) and 55 females with ASD (27 missing; ABIDEII-GU_1 (N=6), ABIDEII-KKI_1 (N=7), Leuven_2 (N=3), ABIDEII-OHSU_1 (N=1), Pitt (N=4), Stanford (N=1), ABIDEII-UCD_1 (N=1), UCLA_1 (N=1), UM_1 (N=3)). [h]ADOS-Gotham RRB was available for 264 males with ASD (98 missing; ABIDEII-GU_1 (N=27), ABIDEII-KKI_1 (N=13), Leuven_2 (N=10), NYU (N=7), OHSU (N=11), Pitt (N=8), SDSU (N=8), Stanford (N=3), ABIDEII-UCLA_1 (N=5), UM_1 (N=6), Yale (N=1)) and 56 females with ASD (26 missing; ABIDEII-GU_1 (N=6), ABIDEII-KKI_1 (N=7), Leuven_2 (N=3), ABIDEII-OHSU_1 (N=1), Pitt (N=4), ABIDEII-UCD_1 (N=1), UCLA_1 (N=1), UM_1 (N=3)). [i]ADOS-Gotham calibrated severity scores [65] were available for 347 males with ASD (15 missing) and 77 females with ASD (5 missing). [j]Attention Deficit Hyperactivity Disorder (ADHD; N=63); anxiety disorder (N=22); Oppositional Defiant Disorder (ODD; N=17); mood disorder (N=11); Tourettes/Tics (N=6); Obsessive-Compulsive Disorder (OCD; N=6); enuresis (N=8); encopresis (N=4); developmental articulation disorder (N=1); developmental dyslexia (N=1); sensory integration disorder (N=1). [h]ADHD (N=17); anxiety disorder (N=7); ODD (N=10); mood disorder (N=2); OCD (N=2); enuresis (N=2); encopresis (N=1). The three group means were compared with ANOVA tests (or Kruskal-Wallis test in the case of non-parametric mean FD) followed by post-hoc pairwise t-test comparisons (or Mann-Whitney U-tests in the case of non-parametric mean FD) when statistically significant (significance cut-off set at $p<0.05$).

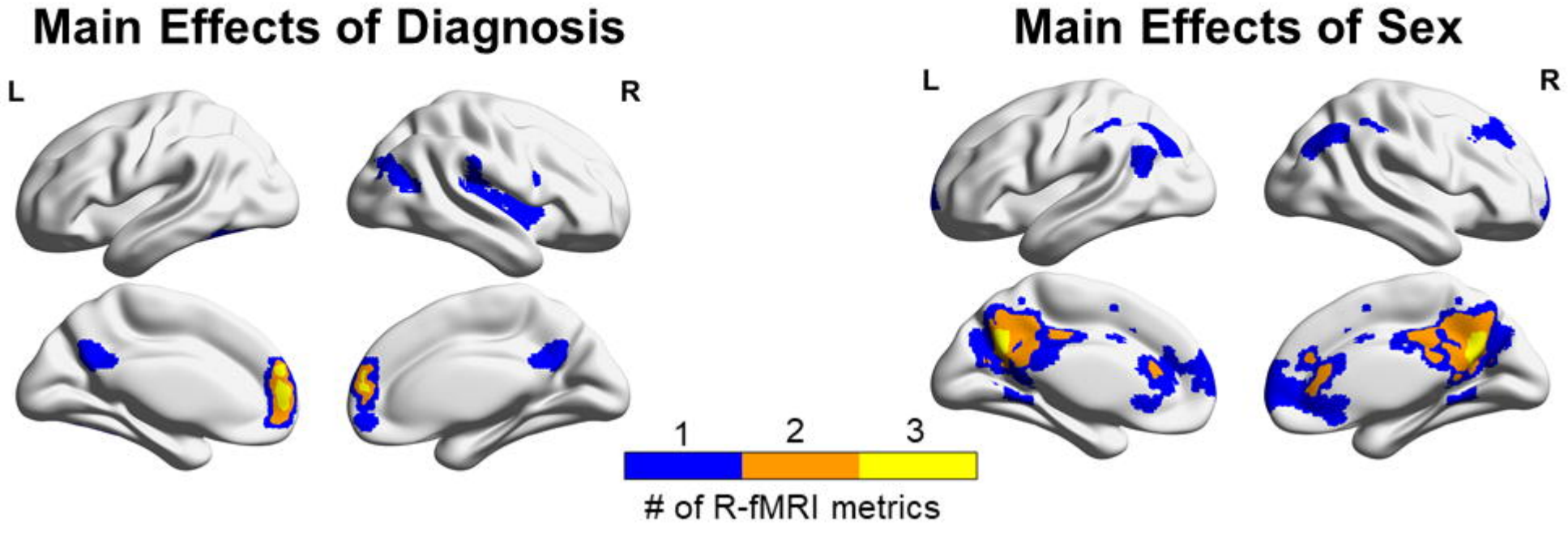

Main effect	Region with overlap	R-fMRI metric		
		PCC-iFC	VMHC	ReHo
DX	Bilateral PCG/FP	■	■	■
Sex	Bilateral ACC	■	■	
	Bilateral PCC/Prec	■	■	■

■ ASD<NT
M<F

■ ASD>NT
M>F

Processing Pipeline

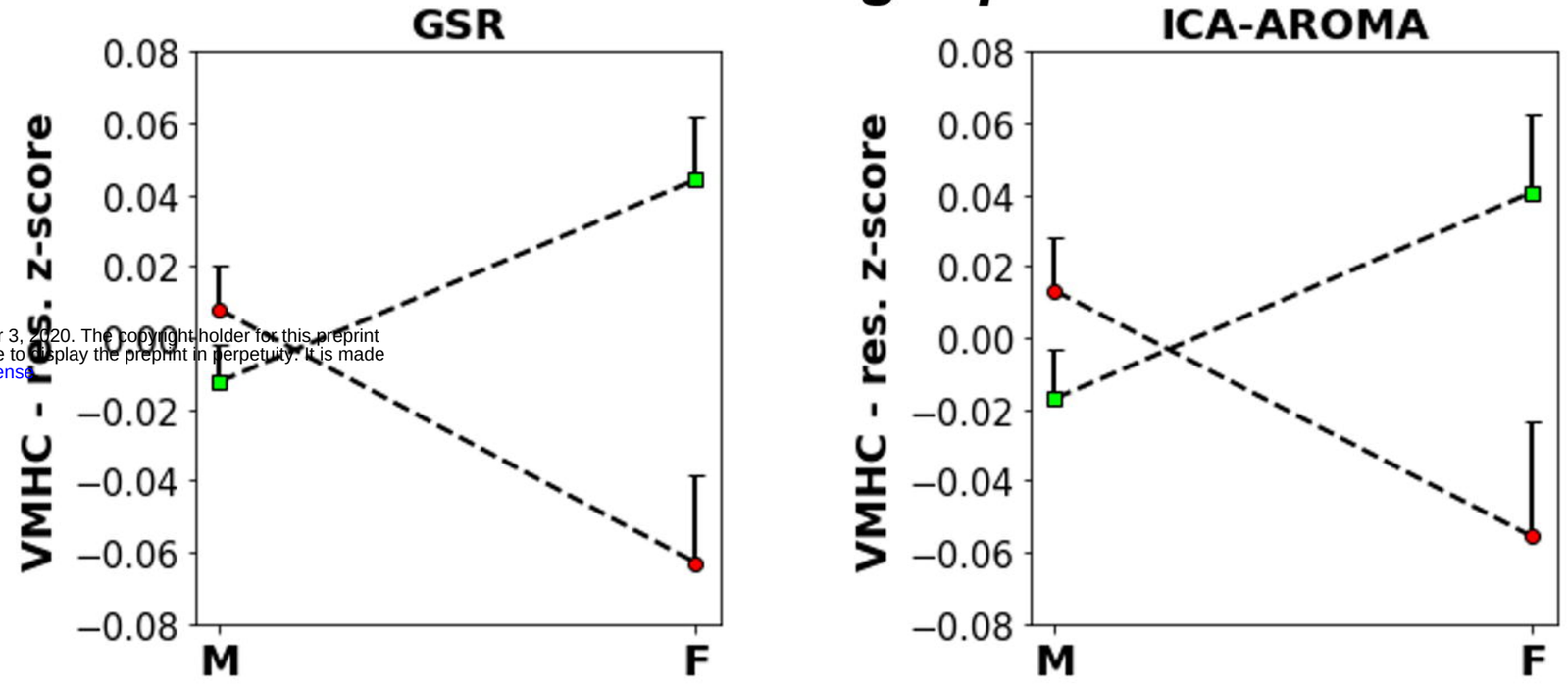

2b

Robustness

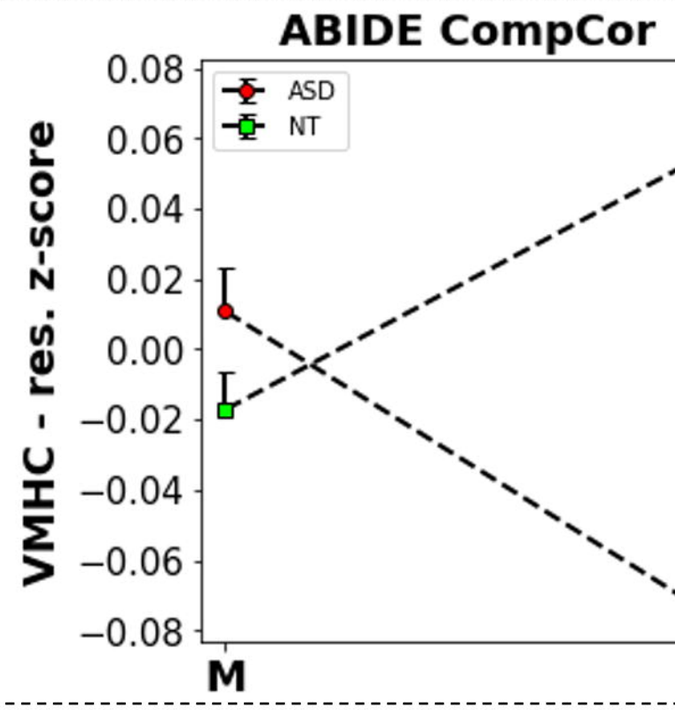

2a

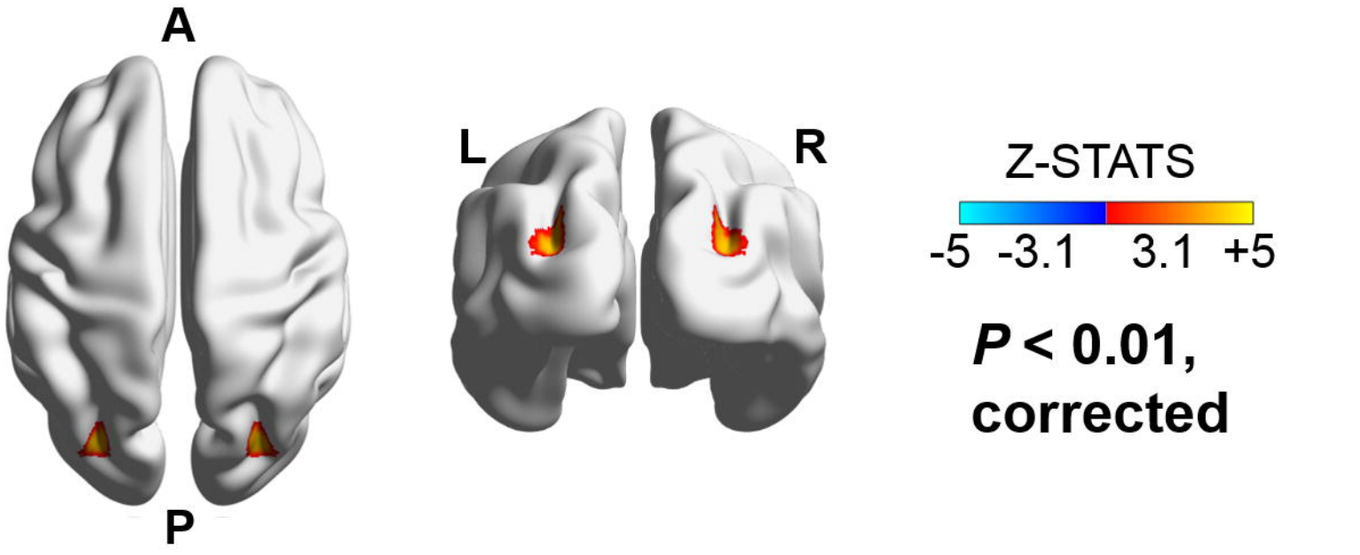

Sample

2c

Replicability

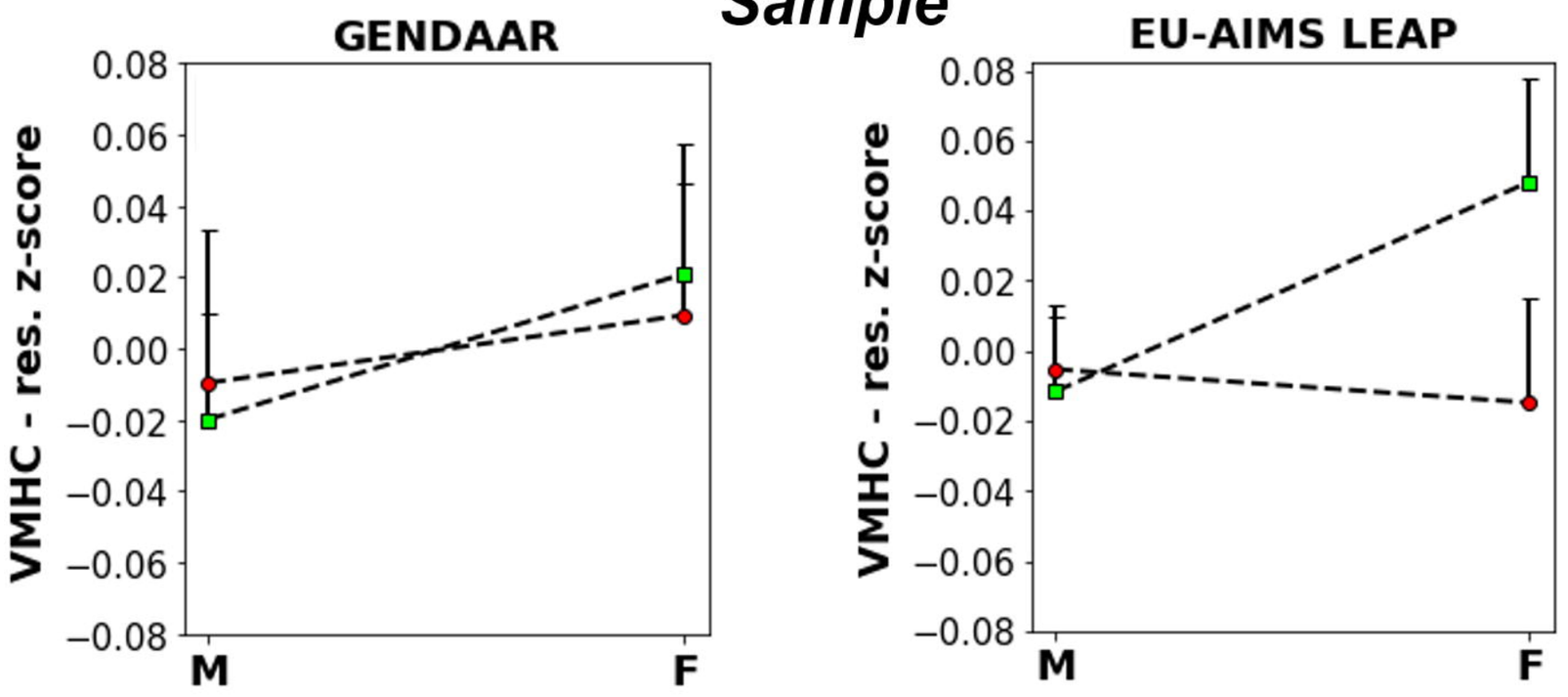

a) Overlap of VMHC cluster with cognitive ontology maps

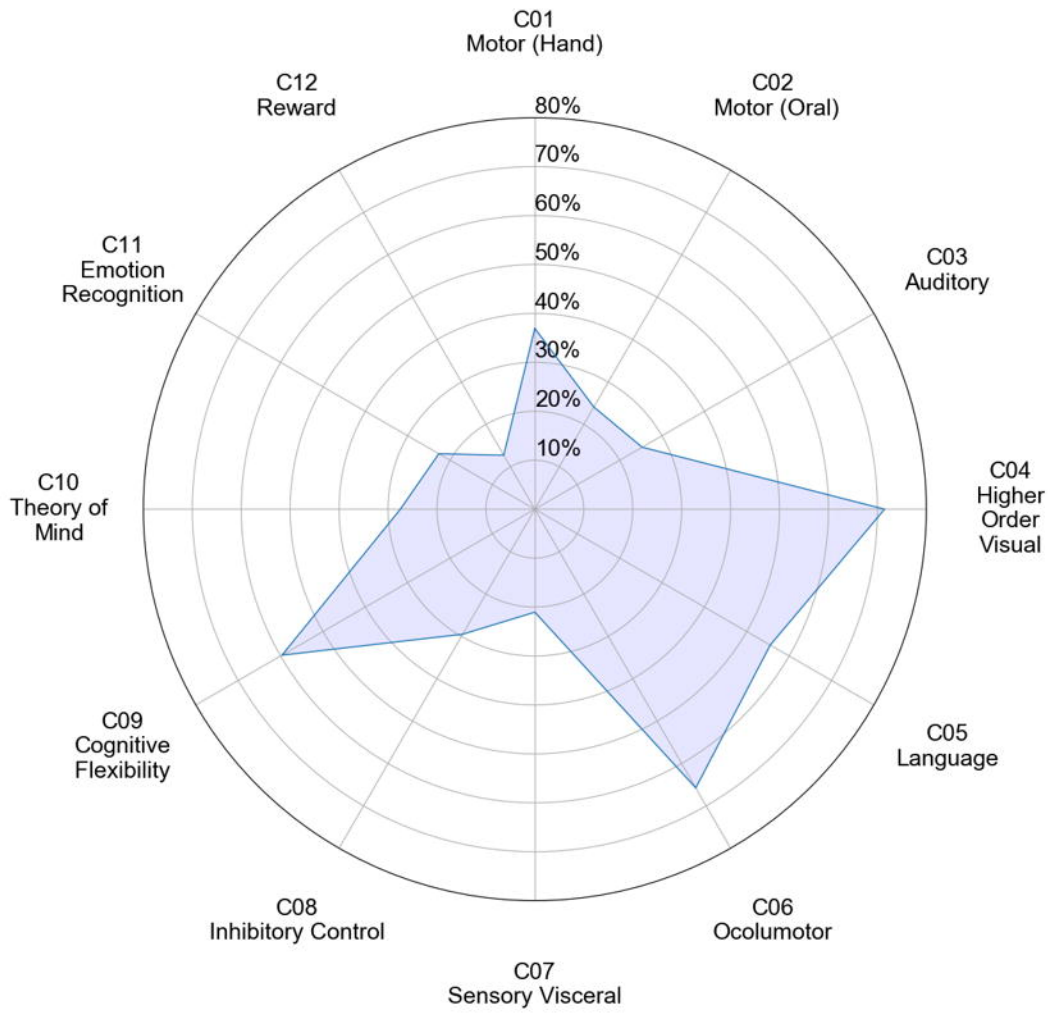

b) Neurosynth terms correlation with VMHC cluster

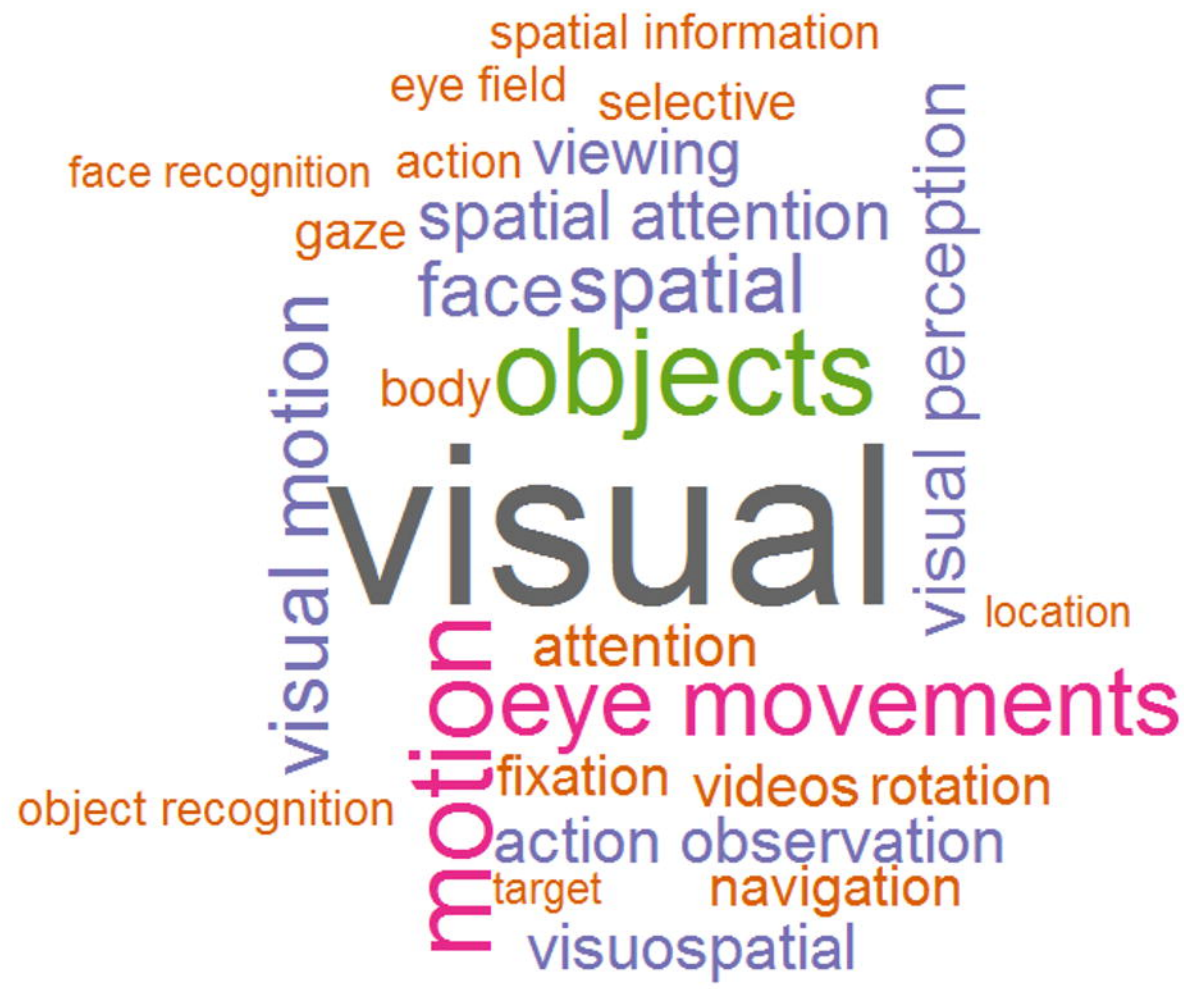

c) Correlation between social-affect ADOS scores and VMHC cluster

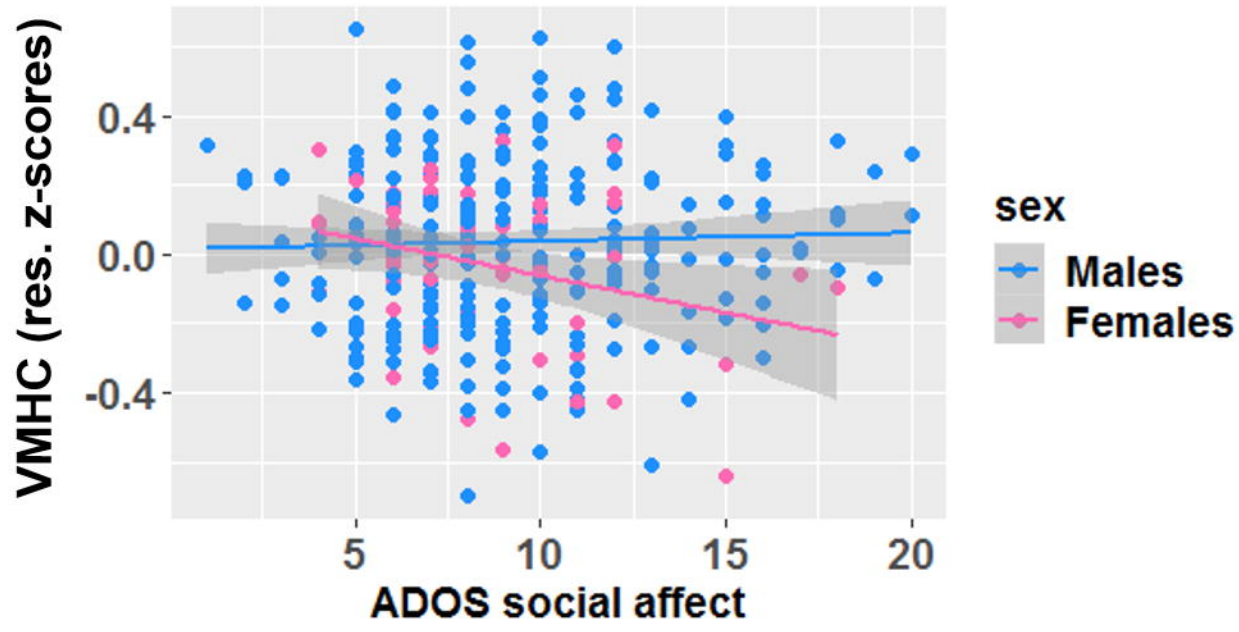

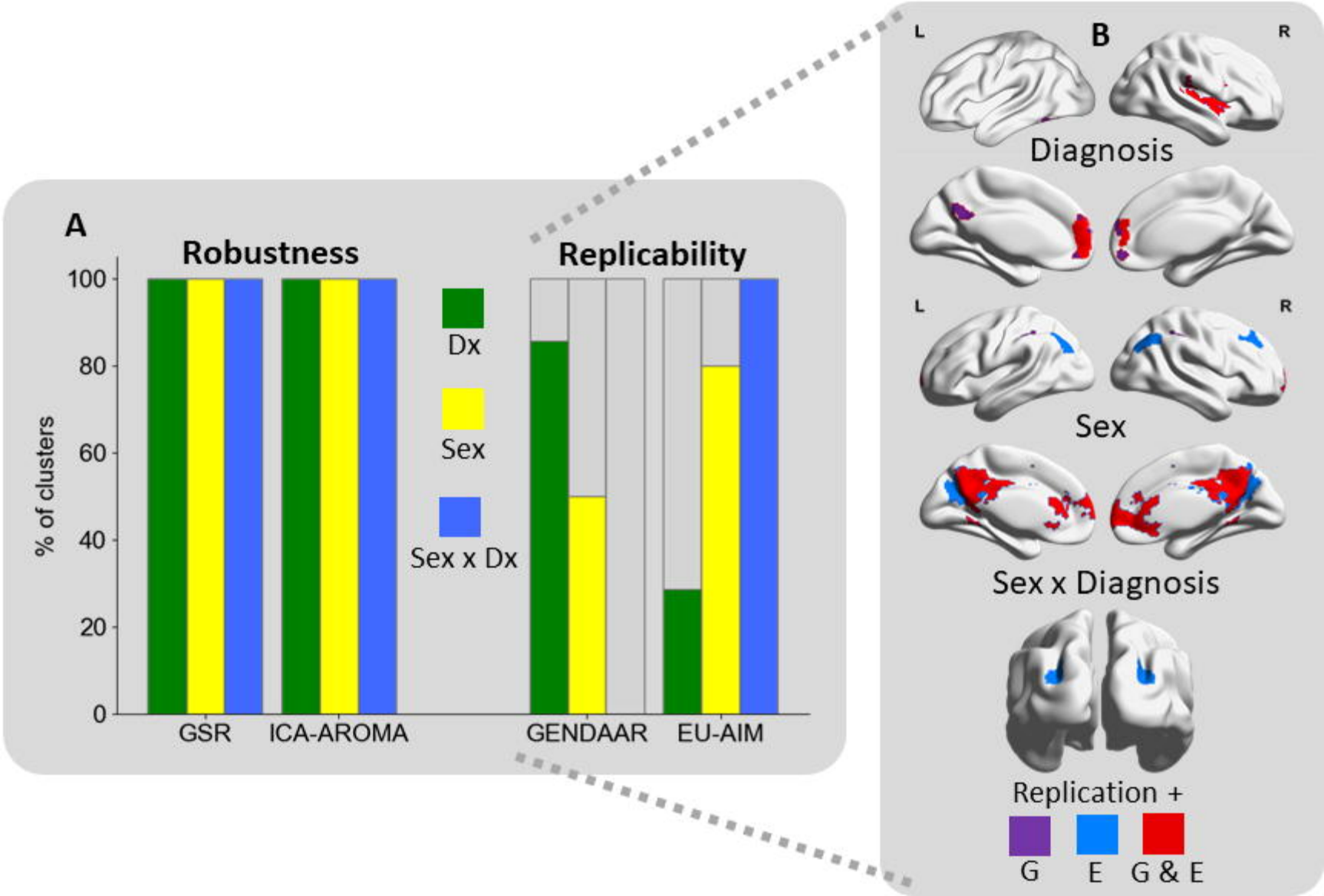
A
Robustness
Replicability
100
80
60
40
20
0
% of clusters
Dx
Sex
Sex x Dx
GSR
ICA-AROMA
GENDAAR
EU-AIM
B
L
R
Diagnosis
L
R
Sex
Sex x Diagnosis
Replication +
G
E
G & E